INVESTIGATION OF THE CHANGE IN THE PHYSICAL PROPERTIES OF NiTi SHAPE MEMORY ALLOYS BY ADDING COBALT ELEMENT

Hanaa Shahab Ahmed ZARDAWI

MSc THESIS

Department of Physics
Supervisor: Associate Prof. Dr. Mediha KÖK

FEBRUARY -2019

REPUBLIC OF TURKEY
FIRAT UNIVERSITY
THE INSTITUTE OF NATURAL AND APPLIED SCIENCES

INVESTIGATION OF THE CHANGE IN THE PHYSICAL PROPERTIES OF NiTi SHAPE MEMORY ALLOYS BY ADDING COBALT ELEMENT

MSc THESIS

by

Hanaa Shahab Ahmed ZARDAWI

(162114104)

Study Field: Physics

Program: Solid State Physics

Supervisor: Associate Prof. Dr. Mediha KÖK

Submitted Date: 18/02/2019

February - 2019

REPUBLIC OF TURKEY
FIRAT UNIVERSITY
NATURAL AND APPLIED SCIENCES INSTITUTE
FACULTY OF SCIENCE
DEPARTMENT OF PHYSICS

INVESTIGATION OF THE CHANGE IN THE PHYSICAL PROPERTIES OF NiTi SHAPE MEMORY ALLOYS BY ADDING COBALT ELEMENT

MASTER THESIS

Hanaa Shahab Ahmed ZARDAWI

(162114104)

Tezin Enstitüye Verildiği Tarih : 14.01.2019

Tezin Savunulduğu Tarih : 18.02.2019

Supervisor : Associate Professor Mediha KÖK (Fırat University)

Jury : Professor Doctor Yakup BALCİ (İnönü University)

Associate Professor Fethi DAĞDELEN (Fırat University)

ACKNOWLEDGEMENT

First, I am grateful to the ***God*** for the good health and wellbeing that were necessary to complete this thesis. I would like to express my gratitude to my supervisor *Assoc. Prof. Dr. Mediha KÖK* for the useful comments, remarks and engagement through the learning process of this thesis. A special thanks also go to my friend *Mr. Ibrahim Nazem Qader* who always helped me and gave me the power for studying. Thanks a lot to *Mr. Muhammed Sait Kanca* who helped me.

Many thanks to my family. Words cannot express how grateful I am to my husband, and all of our family whose acts of supporting me in these times.

I would also like to thank all of my friends who supported me in writing, and incented me to strive towards my goal.

This work has been supported by the Management Unit of Scientific Research Projects of Firat University (FUBAP) (Project Number: FF.18.11).

Hanaa Shahab Ahmed ZARDAWI

TABLE OF CONTENTS

Page No

SUMMARY

INVESTIGATION OF THE CHANGE IN THE PHYSICAL PROPERTIES OF NITI SHAPE MEMORY ALLOYS BY ADDING COBALT ELEMENT

In this study, The NiTi shape memory alloys which doped with 2, 3, 4, 5, and 6 at.% of cobalt element were melted by using arc-melting technique and cooled down to room temperature naturally. To make all contribution elements spread equally in the prepared alloy's ingots, they were kept at 1050 ^{o}C for 24h in a furnace at air atmosphere. By using DSC (Differential Scanning Calorimetry), x-ray diffractometer, optical microscope, SEM-EDX, and PPMS equipment each crystal structure of alloys, the microstructural phases, variation rate in chemical composition, and magnetization properties of the samples determined, respectively. The results showed that alloys with 2, and 3 at.% of cobalt content has martensite phase in room temperature while the others at the same temperature had austenite phase. The enthalpy change found to have different situation for each categories, such that its value increase in martensite phase-alloys, whereas, this value decrease with increasing Co-additive in austenite phase-alloys. Also, magnetization measurement at room temperature showed that austenite phase-alloys have higher magnetization compared with martensite phase-alloys.

Keywords: Phase transformation; Shape Memory Alloy; Cobalt element; Ti_2Ni phase; magnetization properties; NiTi alloy.

ÖZET

Kobalt elementi katkısı ile NiTi şekil hatırlamalı alaşımların fiziksel özellikleri üzerindeki değişimin incelenmesi

Bu çalışmada, atomikçe % 2,3,4,5 ve 6 oranında kobalt elementi katılanan NiTi şekil hatırlamalı alaşımları ark eritme yöntemiyle eritildi ve oda sıcaklığında soğutuldu. Alaşım ingotlarında elementlerin homojen olarak yayılması için 1050 ^{o}C de 24 saat fırında hava atmosferinde bekletildi. Alaşımların dönüşüm sıcaklıkları, kristal yapıları, mikroyapısal fazları, kimyasal oran değişimleri ve manyetik özellikleri, DSC (Diferansiyel Taramalı Kalorimetre), x ışınları difraktometresi, optik mikroskop, SEM-EDX cihazı ve PPMS (fiziksel özellik ölçüm cihazı) kullanılarak belirlendi. Sonuçlara göre, atomikçe %2 ve %3 kobalt içeren alaşım, oda sıcaklığında martensit fazda, diğerleri ise austenit fazdadır. Entalpi değişimi bu iki durum için farklılık göstermiştir. Martensit fazda olan alaşımlarda artmış, austenit fazda olan alaşımlarda azalmıştır. Bu azalış, austenit fazda olan alaşımlarda Co katkısını artmasından kaynaklanır. Bununla birlikte oda sıcaklığında alınan manyetizasyon ölçümlerine göre, austenite fazda saturasyon değeri, martensit fazdaki alaşımlara göre daha yüksektir.

Anahtar Kelimeler: faz dönüşümü; şekil hatırlamalı alaşım; Kobalt element; Ti_2Ni faz; manyetizayon özellikleri; NiTi alaşımı

TABLE OF FIGURE

Page No.

LIST OF TABLE

Page No.

ABBREVIATIONS

RT : Room Temperature

A : Austenite phase

M : Martensite Phase

A_s : Austenite start temperature

A_f : Austenite finish temperature

M_s : Martensitic start temperature

M_f : Martensite finish temperature

Co0 : $Ni_{50}Ti_{50}$ alloy

Co2 : $Ni_{48}Ti_{50}Co_2$ alloy

Co3 : $Ni_{47}Ti_{50}Co_3$ alloy

Co4 : $Ni_{46}Ti_{50}Co_4$ alloy

Co5 : $Ni_{45}Ti_{50}Co_5$ alloy

Co6 : $Ni_{44}Ti_{50}Co_6$ alloy

SMA : Shape Memory Alloy

SME : Shape Memory Effect

SE : Superelasticity (Psu-elasticity)

XRD : X-Ray Diffraction

DSC : Differential Scanning Calorimetry

EDX : Energy Dispersive X-ray

SEM : Scanning Electron Microscope

Ni : Nickel

Ti : Titanium

Co	:	Cobalt
Fe	:	Iron
Pd	:	Palladium
Nb	:	Niobium
Hf	:	Hafnium
Pt	:	Platinum
Zr	:	Zirconium
Mo	:	Molybdenum
Al	:	Aluminum
NiTi	:	Nitinol alloy
T_o	:	Equilibrium temperature
G^M	:	Gibbs free energy in martensite phase
G^A	:	Gibbs free energy in austenite phase
H^M	:	Enthalpy in martensite phase
H^A	:	Enthalpy in austenite phase
S^M	:	Entropy in martensite phase
S^A	:	Entropy in austenite phase
ΔT	:	Change of Temperature
$A \rightarrow M$	:	Austenite to Martensite transformation
$M \rightarrow A$	:	Martensite to Austenite transformation
at. %	:	Atomic percentage
aw. %	:	weight percentage

1. INTRODUCTION

The modern engineered equipment in different areas always replaced with new technologies that have more efficiency and comparably lower cost. Material properties have been the key point in most cases. There are a limited known chemical elements found, which has a defined features, whoever, there are several techniques that can be utilized to alter their properties. Another materials that have being used from bronze-age till now, are alloys. Alloys are composite of at least two different composition elements that shared their physical property in the new product. These kind of materials usually is the most popular materials among material scientists. Since, adding different ratio, different element, heat treatment, and mechanical treatments can be used for modifying alloys, then it gives a wide area to researchers to check out any techniques in this list.

Shape memory alloys (SMAs), have specific properties that distinguished them from the other alloys. In a particular range of compositions, they have different crystal structure which can switch with changing temperature. The higher and lower temperature phases that are, respectively, known as austenite and martensite phases can change the values of most physical properties of the alloy. Ability to return the first shape is the most important characteristic of these alloys.

There are thousands of research that tried to produce different transformation temperatures, temperature hysteresis, improving magnetization, and thermal stabilities of SMAs [1-3]. J Khalil-Allafi et al. [4] aged NiTi alloy, and they found the effect of aging on phase transformation temperatures. Aging led to growth Ni_4Ti_3-precipitates, and thus, the austenite finish temperature shifted to higher temperature. Likewise, Danuta Stroz and colleagues [5] conducted a study for the effect of aging 400, 500, 600 and 700 ^oC for 1 h on Ni-Ti alloy. They notice that aging at 500 ^oC at causes to precipitate Ni_4Ti_3 phase and thus M_s temperature increased due to decreasing in Ni-composition. In a different study, J. Otubo et al. [6] found the effectiveness of different chemical composition and carbon/oxygen doped elements on enthalpy and temperature hysteresis of NiTi alloy. Also, Mediha Kök et al. [7] used oxidation to improve the surface of NiTi SMA. According to C.W.Gong et al. [8], Tantalum addition in NiTi alloy caused to produce soft β-Ta phase, and hence, the martensite stabilization of Ni-Ti-Hf became higher than NiTi SMA.

The current study has been organized such that in chapter 2 deal with historical and achievements of shape memory alloys (SMA). Then the SMA has defined carefully and their special properties with some diagrams illustrated. Moreover, the application in different areas explained. Also, some modification of NiTi alloys in term of additional element and their physical influences have given. In the third chapter the experimental procedure clearly explained. The results of different measurements such as DSC, XRD, EDX, SEM, OM, and magnetization analyzed and compared with literature in chapter 4. Finally, in some pullet points the important results of this study summarized.

2. SHAPE MEMORY ALLOYS

2.1 History of shape memory alloys

Ölander, Swedish physicist, was the first how observe the shape memory effect (SME) in gold-cadmium, Au-Cd. In 1932 he realized that the plastic deformation accrued in room temperature could be recovered without any cold or worm work on it [9]. Six years later, in 1938 SME had found in each copper-zinc (Cu-Zn) and Copper-tin (Cu-Sn) binary alloys [10].

The discovery for finding new alloys that could exhibit SME continued until in 1962 both William Buehler and Frederick Wang checked out this effect on NiTi [11]. Their specimen alloy was fortunately showed a best result and it has become a wanted material in many commercial purposes [12]. The alloy got a nickname in markets, were called NiTiNOL. There were many advantages of NiTi alloys that overtaking their competitors e.g. lower cost producing, safer for health and easy to use, also their mechanical features were comparably suitable than the other shape memory alloys which were known at that time [13].

Since manufacturing factories needed smart materials to enhance their products, in 1969 SMAs for the first time utilized as a smart materials for pipe coupler in hydraulic lines which embedded in the motors of F-14 jet fighter refers to USA military army [14]. After aerospace, in 1971 the SMAs got inside the orthodontic filed. Before that time, the materials that had being used had some technical problems that were talked by nitinol alloys [11]. NiTi alloys have lower stiffness, could exert a constant force due to phase transformation, and have a longer effective strain recovery. Likewise, the compatibility and lower weight of NiTi alloys were opened the gate of other areas.

2.2 Definition of a Shape Memory Alloy

Shape Memory Alloys (SMAs) are alloys that have different temperature dependent phases, which have ability to remember a given form in its higher temperature, and when they loss their prior shape due to plastic deformation, just by switching their phases by heating process one could achieved approximately the first fabricated shape. Therefore, for ant SMAs the higher and lower temperature phases are called austenite and martensite, respectively. While they have the same entities in their lattices, but they have different physical properties because of their variety of atomic arrangement. Some properties of these phases for particularly nonferrous SMAs are listed in Table 2.1.

Table 2.1. Definition of austenite and martensite phase [11].

Martensitic	Austenite
• Lower temperature phase	• Higher temperature phase
• Monoclinic Crystal Structure	• Cubical crystal structure
• Could be either exist in either twining or detwining microstructure.	• Twining is not happened in its phase.
• During cooling austenite phase starts transform to martensite phase at M_s and transformation completed at M_f.	• During Heating martensite phase starts transform to austenite phase at A_s and transformation completed at A_f.

2.3 Shape memory effect

Shape memory effect, SME, is an appearance of thermoelastic martensitic transformation, which is a nucleation independent conversion. The SME is a phenomenon that a SMA return back to its predetermine shape through heating. This Property is the outcome of reversible phase transformation in SMAs. SME is based on martensitic-austenite, austenite-martensitic transformation after applied heat or stress.

SME are classified to two common classes which depend on the direction of recovery. One way shape memory effect, OWSME, that is happens for SMAs that have only one recoverable shape in higher temperature, however, there are also have two way shape memory effect, TWSME that in each phases could memorize two different shapes.

2.3.1 One-way shape memory effect (OWSME)

The one-way SMA (OWSMA), after the removal of an external force can be keep a deformation state, and then recovers to its main shape upon heating. It is important to note the material suppose that the same shape in both austenite phase and martensitic phase except if it is deformed the martensitic phase and macroscopic change occurs between the phases in one way SME [15].

2.3.2 Two-way shape memory effect (TWSME)

In this way the material remembers both a high and a low temperature shape. 'Two-way' shape memory (TWSM) effect happen when there is a spontaneous shape change of a material on both heating and cooling. In TWSM, no external force is wanted to be obtained any shape change, and the sample simply curvature in two different ways upon heating or cooling. Perkins and Hodgson enumerate various applications of the TWSM [16]. The first report of TWSM was by Wang and Buehler [17].

2.4 Superelasticity

Superelasticity is the shape memory property that has been most exploits for business use. Superelasticity behavior at temperature above A_f and lower than M_d can recover a large deformation simply by releasing the applied force .These materials have the ability to undergo a big deformation when load is applied at specific temperatures and get back to their original morphology when unloaded. shape memory alloys can be two different phases and three different crystal structures (twinned martensite, detwinned martensite, and austenite)[18, 19]. The austenite and martensite have stability property in high and low temperature, respectively. However, superelasticity is limited to the temperature range $A_f < T < M_d$ and a critical stress, which are, in sure, depends on the material property.

Figure 2.1 shows the stress vs. strain (σ - ε) to illustrate the superelasticity of SMAs. As all metallic material, SMAs also, have elastic property. The (1) part of Figure 2.1 shows the linearly relation of σ – ε which its slope define the stiffness. Furthermore, the (2) part is a plateau that with a constant applying force the SMA elongate due to phase transformation from austenite, stable phase, to detwinned martensitic, unstable phase. Then, when the metastable martensite created, by increasing load the material again show another elastic deformation, but in the martensite-based microstructure (3). After that, if superelastic material unloaded, the elasticity recovered, which is portion (4) illustrated in Figure 2.1. Then through portion (5) the unstable martensite transforms to austenite phase and, finally, the austenite phase elastically return back to its original shape, first portion.

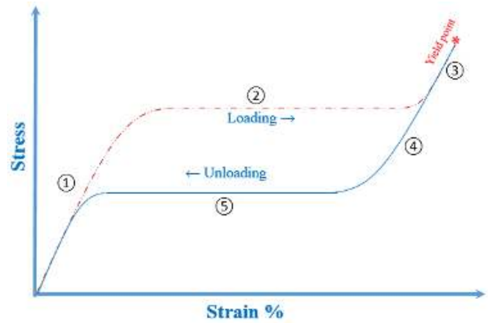

Figure 2.1 schematic stress-strain relationship of superelastic SMAs [15].

2.5 Applications of shape memory alloys

Shape memory alloys are widely used in the many fields. The nature of shape memory recovery and transformation has been selectively explored for commercial applications. The categorizations fall into the following broad groupings:

2.6 Free recovery

These are applications based on the ability of the material to deform in its martensitic state and recover its original shape when heated to temperatures above the transformation temperature thereby recovering the deformation strain. These applications employ thermoelectricity and notable applications are in blood clot filter, self-expanding stents and atrial septal defect occlusion device used for sealing hole in heart walls [20].

2.6.1 Robotic applications

As it were shown that SMAs could restore the strain due to phase transformation, then they could be a good candidates for producing SMA-based actuators. However, since the displacement that they can move are approximately less than one centimeter, so these kind of actuators could be utilized in mini machines and robots that their motion based on crawling, jumping, flowing, walking, and in addition the robots that handled for fabricate medical instruments and biomimetic robots.

As it were shown that SMAs could restore the strain due to phase transformation, then they could be a good candidates for producing SMA-based actuators. However, since the displacement that they can move are approximately less than one centimeter, so these kind of actuators could be utilized in mini machines and robots that their motion based on crawling, jumping, flowing, walking, and in addition the robots that handled for fabricate medical instruments and biomimetic robots.

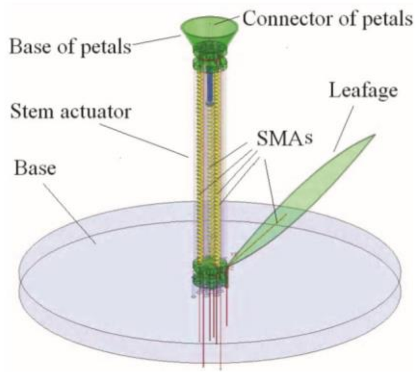

Figure 2.2 Schematic diagram of flower robot [21].

Flower robots, as an example, are one of simplest automation device that similar to the natural flowers, have leaves, petals and stem [22]. They equipped by sensors and actuators that could react with the environment. At 200 and 2008 Huang et al. [21] were the first investigators who developed SMAs for designing and atomized flower robots. The most functionality of their flower were blooming petals by detecting light, twisting leaves by blowing wind, and shaking the stem. Figure 2.2 shows the sketch of flower robot with SMAs embedded in its leaf and stem, and other smart materials also have roles in building block of this intelligent flower.

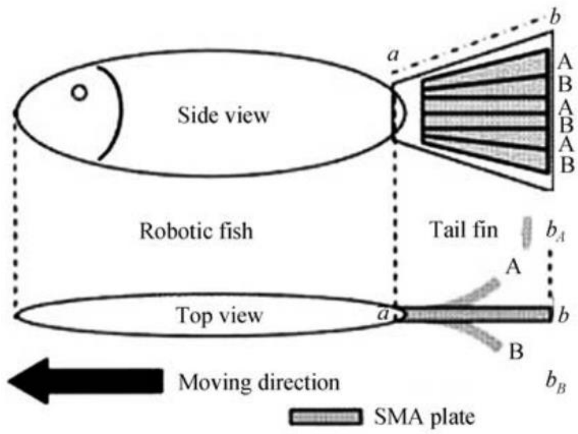

Figure 2.3 Robotic fish with caudal peduncle actuator [23].

In addition, fish robots are another fabricated animals that used many parts of their body to have a swimming-like locomotion. Tao et al (2006) from University of Washington [23], suggested a caudal peduncle actuator based on ferromagnetic shape memory alloy, FSMA, is illustrated in Figure 2.3.

Steps of working this actuator are as follows:

1. Appling an external magnetic field;
2. A stress field will be induced in the actuator;
3. Phase transformation is occurred from austenite phase to martensite phase;
4. Due to this phenomenon, which is called strain induced martensite (SIM), the material become softer, and hence caused a moving the robot.

This concept, also, has been used in synthetic jet actuator (SJA) as membrane that could produce high velocity jet flow (190m/s) and working with a frequency of 220 Hz. It is comparably better than piezoelectric that eject jet flow with 100m/s and in frequency around 300Hz [24].

Walking is one locomotion method that some animal used for changing their position. This is also has been handled in some robots that were given some particular tasks. In 2006 Nishida et al [25], introduced walking robots based on SMAs, which possessed four degree of freedoms. Their robot had two legs that constructed from a flat polyethylene plate and SMAs embedded inside them. They used two abilities, which were elasticity of polyethylene and shape recovery of SMA. There are two statuses that result walking of the robot Figure 2.4.

- Polyethylene has no elastic potential energy to release and it is situated at its ordinary shape.
- The martensite phase of SMA is deformed and creates a detwinned martensite.

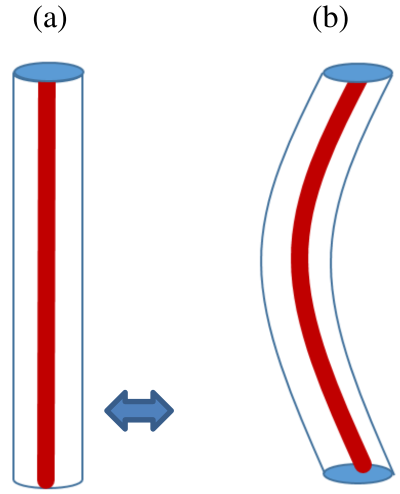

- Due to heating the martensite phase of SMA transform to austenite phase and hence recover its original form, which is a bending shape.
- Polyethylene is a flexible material, so it elastically deform and due to this deformation it saves a potential energy.

Figure 2.4 Schematic diagram of walking-robot leg [22].

2.6.2 Smartphone Fabrication

Nowadays, smartphones are one of the most popular gadgets among people that smart materials played an important role in its fabrication. They have much functionality not only in variety in their software program applications but also in each hardware components. To reduce the impact of falling, the smartphone's morph can changed to ring-like shape. To achieve this futuristic property SMAs are the best nomination to design these kinds of mobiles. The SMAs are taken in some orientations in a flexible body and are given some predetermined shape. Thus, when the accelerated sensor measured the free fall status of smartphone, it will send a signal to SMAs to go to emergency situation form, which is a tube like shape.

Moreover, SMAs could be controlled to give a notification by changing the shape of smartphone to some abnormality. For instance when a massage received it could make a wave in the form. This method could be replaced to sound or light warning.

2.6.3 Biomedical applications

Some robots that can creep like inchworm, which can be used for colonoscopy and inspection of colon's diseases. In 1999 Reynaerts et al [26], proposed a robot with bending, elongation and clamping modules all based on SMAs, Figure 2.5. During expansion (contraction) backward (forward) clamping actuators activated and the others being deactivated. Thus, the robot moves entirely forward. Also, bending actuator can be used for turn inside colon. That prototype was more powerful than the other robots with the same size.

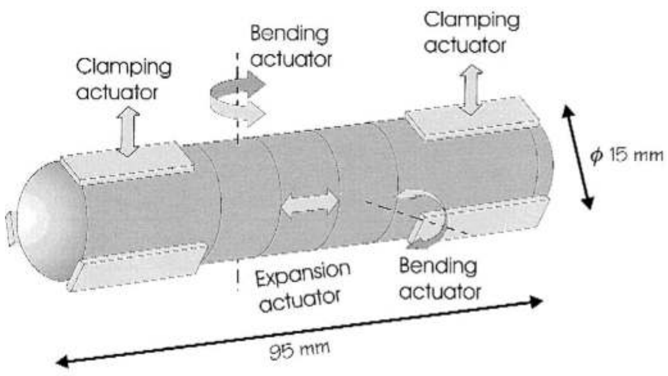

Figure 2.5 Inchworm-like robot with three various functional actuators [26].

In 2004 Menciassi et al. developed the idea to construct earthworm-robot that its actuators was based on SMAs, and they tried to design it in a real size [27]. Their robot had four modules of actuators and all inserted in a silicon sell, which mad it become softer and more efficient for colonoscopy, as shown in Figure 2.6.

Figure 2.6 The prototype of earthworm robot [27].

Smart materials in general and SMAs particularly given an opportunity to design human body for different purposes. One of the proposed human bodies is a hand with different number of fingers, Figure 2.7, which were developed by many researchers [28-32].

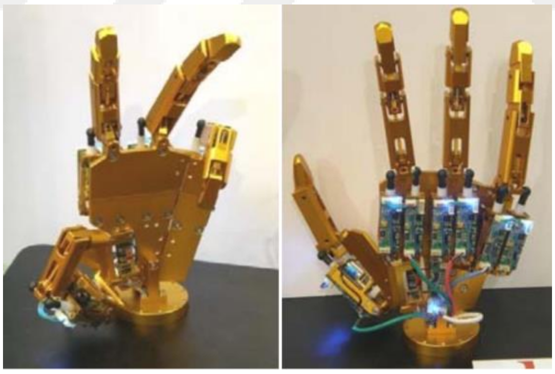

Figure 2.7. A prototype of a robot hand in various forms [28].

2.7 Shape morphing of aircraft wing

SMAs are those materials that have been added to the list of DARPA Smart Wing program. It is aimed to build an aircraft wing by using smart materials. Two different oriented actuators which made of SMAs connected in heads and their tails connected to top and bottom of flexible wing, Figure 2.8. However, there are some challenges that reduced the efficiency of these actuators, whereby, after passing some cycles they could not recover trailing edge tip of the wing to the determined form [33].

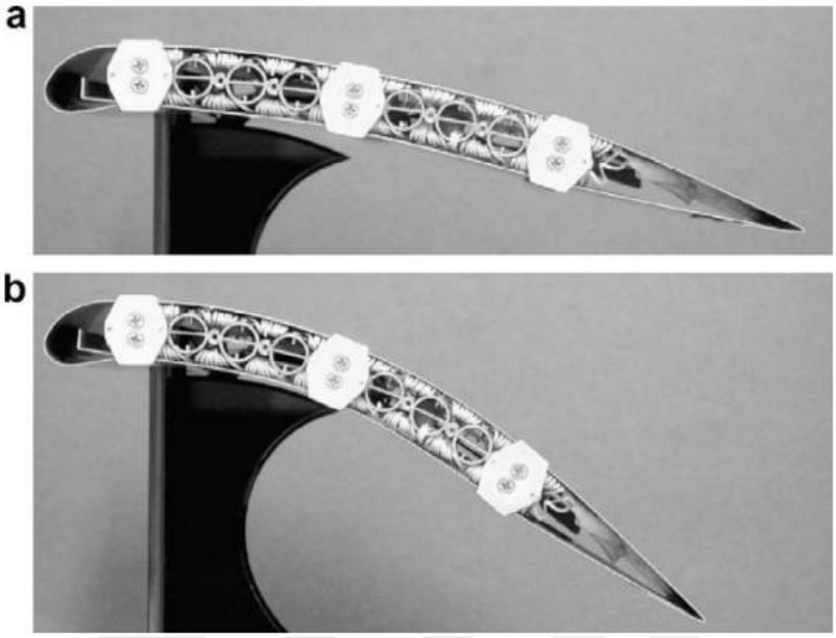

Figure 2.8 (a) first (b) second morph of prototype wing that witch its morph due to heating the SMA-actuators [34].

2.8 NiTi shape memory alloy

The most popular shape memory alloy is nickel-titanium alloy, (NiTi). NiTi alloys exhibit one- and two-way shape memory effects and superelasticity, they are classified as intelligent materials. Shape memory effects are related to reversible, thermoelastic martensitic transformation that occurs in these alloys when they are heated to a specific temperature, $>A_f$, and then cooled them down to suitable temperature, $<M_f$, , whereas superelasticity is associated with phase transformation induced by an external stress at temperature range ($A_f < T < M_d$) [35].

Approximately equal atomic NiTi alloys are highly demanded for their unique shape memory characteristics in engineering applications. Among the shape memory alloys, NiTi shape memory alloys are highly demanded for their low elastic anisotropy, high stabilization properties, excellent mechanical properties and good corrosion resistance. In Table 2.2, most important physical and mechanical properties of NiTi are listed [36].

Table 2.2. Some physical and mechanical properties of NiTi alloys [33].

Property	Some properties	Values
Physical	Melting point	1340 ^oC
	Density	6.45 g/cm^3
	Thermal Conductivity	Austenite phase:0.18 W.cm/^{o}C Martensite phase:0.086 W.cm/^{o}C
	Thermal expansion coefficient	Austenite phase:11x10^{-6} /^{o}C Martensite phase: 6.6x10^{-6} /^{o}C
	Heat Capacity	0.20 cal/g ^{o}C
	Electrical Conductivity	$0.5\times10^{-6}\Omega m$
Mechanical	Young moduli	Austenite phase:83 GPa Martensite phase: 28-41 GPa
	Poisson rate	0.33

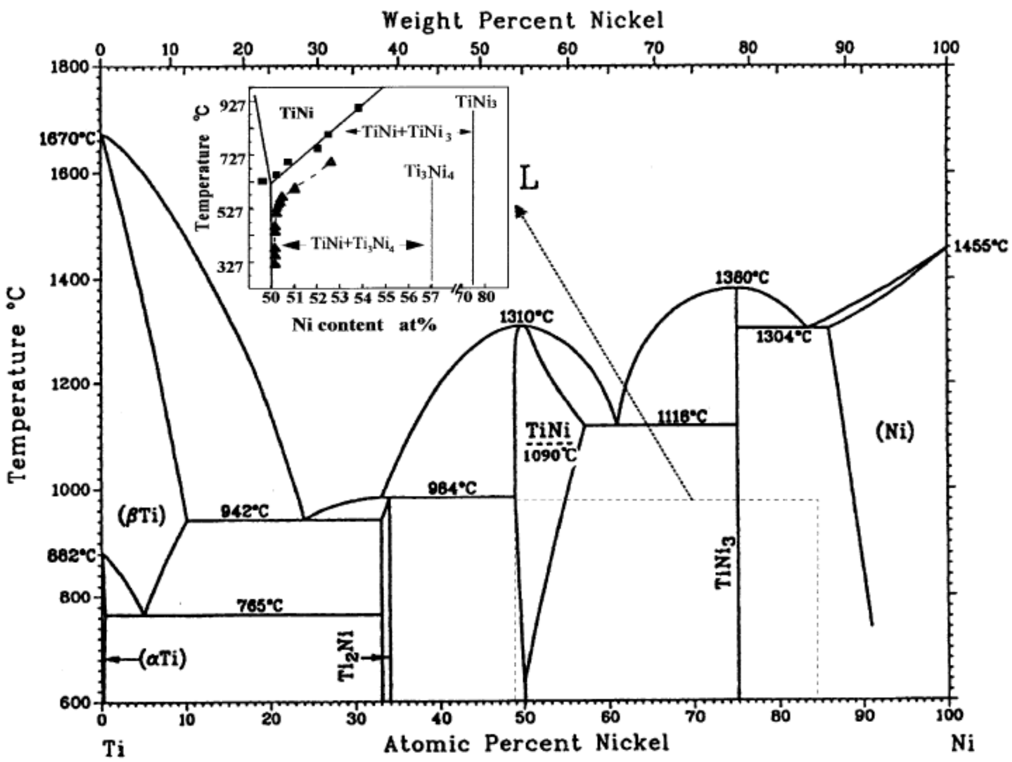

Figure 2.9 The phase diagrams of binary NiTi alloys [37].

2.8.1 Phase diagram and Crystal structure of NiTi Shape memory Alloys

There are several phases could be seen in phase diagram of NiTi alloys. The change of phases by composition and temperature are shown in Figure 2.9. The transformation temperatures decrease strongly with increasing of Ni content. The high-temperature phase (austenite) has an ordered bcc structure (B2), also the low-temperature phase (martensite) has an ordered monoclinic structure (B19′) [38].

NiTi alloys may exhibit three phase structures. The high temperature phase is the austenite phase, and due to cooling process the phase can be transformed to R-phase and martensite phase. Figure 2.10 shows these three phases, where the red and green circles denote the Ni and Ti atoms, respectively [39].

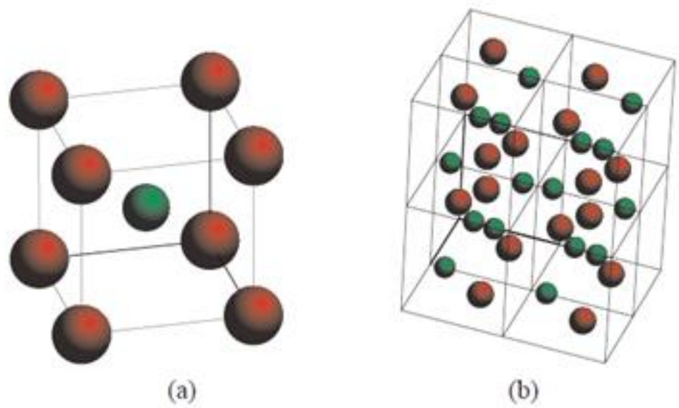

Figure 2.10 a) B2 Cubic (Austenite), b) B19 monoclinic (martensite), c) R rhombohedral phase crystals that can form in NiTi [40]**.**

The austenite phase has B2 crystalline structure with two atoms in the unit cell. Also, the martensitic phase (B19′) is a monoclinic crystalline structure. In addition, R phase has rhombohedral crystalline structure [37]. During cooling, the R phase can be seen before the martensite phase. The transformation takes place as follows: (A → R → M). During heating, the R phase occurs before the austenite phase. The transformation takes place as follows: (M → R → A). Therefore, the R phase can be observed under any condition. Likewise, R phase may be formed by doping the third element into the NiTi alloy or by heat treatment at 400-500 °C [16].

NiTi alloys are often demanded for equal atomic alloys, which mean they have the same atomic rate. In NiTi phase diagram, the compound $NiTi_2$ is intermetallic phase and named as Titanium rich phase, also, Ni_3Ti is named as Ni-rich phase. Ni-rich phase region can be increased by either rising temperature or heat treatment. Nickel-rich regions each Ni_4Ti_3 and Ni_3Ti_2 phases produced (Figure 2.9). $NiTi_2$ phase is rich in Ti-rich region and

Ni_3Ti, Ni_3Ti_2, Ni4Ti3 precipitates in the Ni-rich region significantly and mechanically and functionally affect [41].

Table 2.3 Summary of the crystallographic information on various phases found in Ni-Ti alloy system [41].

Phase	Crystal Structure	SG (atoms / unit cell)	Lattice parameters
NiTi Austenite	Cubic B2	Pm-3m	a = 3.015 Å
NiTi Martensite	Monoclinic B19′	$P2_1/m$	a=2.898Å, b=4.108Å, c=4.646Å, $\beta = 97.78°$
$Ni_{40.5}Ti_{49.5}Cu_{10}$	Orthorhombic B19	Pmma	a=2.881Å, b=4.279Å, c=4.514Å,
NiTi (R-Phase)	Trigonal	P3 or P-3	
Ti_2Ni	Cubic	Fd-3m	a=11.32Å
Ti_3Ni_4	Rhombohedral	R3	a=6.70Å, $\alpha = 113.8°$
Ti_2Ni_3	Tetragonal, Orthorhombic	I4/mmm Bbmm	a=3.095Å,c=13.585Å a=4.398Å,b=4.370Å, c=13.544Å
$TiNi_3$	Hexagonal DO_{24}	$P6_3/mmc$	a = 5.1010 Å, c=8.3067 Å

There is more explanation about existence phases in Ni-rich NiTi alloy as follows:

a. Ti_3Ni_4: Ti_3Ni_4 is a very important phase. Since this phase affects the shape memory characteristics in Ni-rich Ni-Ti alloys.

b. *Ti_2Ni_3:* As discussed above, Ti_2Ni_3 is the second metastable precipitate that forms at intermediate temperatures or at low temperatures for longer aging times.

c. *$TiNi_3$:* Taylor and Floyd investigated the structure of $TiNi_3$ and reported a hexagonal DO_{24} type ordered structure with space group $P6_3/mmc$ [41].

2.9 Uses of NiTi

Shape memory alloys are a set of metallic materials with some remarkable properties like one-way and two-way shape memory effects, superelastic effect, high damping property and rubber-like effect. These characteristics make the material proper for different orthopedic applications such as load-bearings, plates for bone fracture repair, internal fixators for long bone shafts, spinal correctors, vertebral spacers and bone distraction devices. Some of these applications are explained in the following subsections.

2.9.1 Medical Applications

2.9.1.1 Dental application NiTi

For solve the problem of misaligned teeth, a physiotherapy method has being suggested by using orthodontic wire. At the beginning gold alloys were commonly used. After that stainless steel stepped on to this kind of appliance. Next, arch wires were mad of beta titanium and Cr-Co-Ni alloy introduced to the field [42, 43].

In the recent years, NiTi alloy, which has superelasticity property and lower elastic modulus than the other counterparts, are popularly using. In addition, its lower stiffness behavior, allows fabricating wires with rectangular cross sections that could help further moving of teeth. Also, The range of constant force can be changed by either heat treatment or rate of compositions [44].

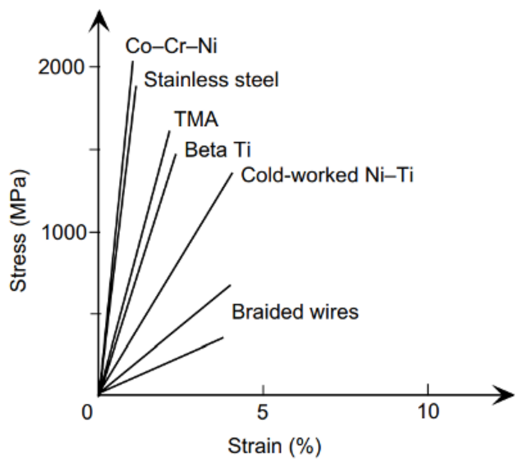

Figure 2.11 Stress–strain relationship for several metallic alloys that have being used for orthodontic issues [44].

Figure 2.11 illustrates the stress-strain curves of main metallic alloys that were utilized for misaligned teeth. Some ones, i.e. stainless steel, have a huge elastic deformation (

Figure 2.12a), while their stiffness makes some limitation to use. On the other hand, there are alloys, i.e. NiTi, have lower elastic moduli (

Figure 2.12b), however their effective strain range are bigger. The applying force is classified to excessive, optimal, suboptimal, and subthreshold. The excessive force zone can damage the tissue, also a suboptimal force may reduce the efficient treatment and with more reducing the force the induced stress drops to subthreshold zone, where the force has not make an affective movement. The utilized range is optimal zone that is used for orthodontic therapy.

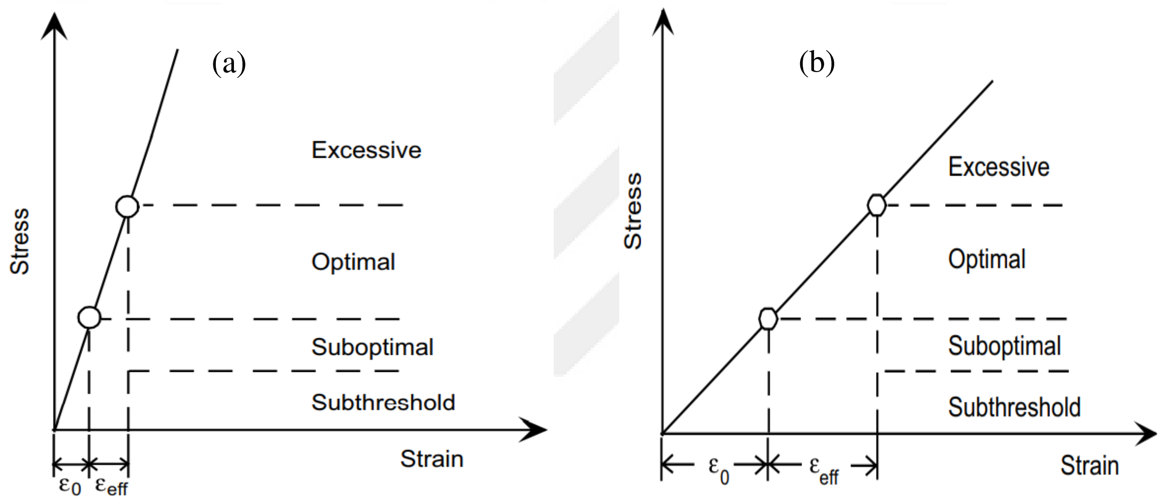

Figure 2.12. Schematic diagrams of stress–strain relationship for, (a) alloy with high elastic modulus, and (b) lower elastic modulus [44].

As it is known, NiTi has a superelasticity property due to phase transformation in an isothermal process. The martensitic phase created between $A_f < T < M_d$ is an metastable phase and when the external force removed it tried to recover the strain be transform to parent (austenite) phase. The advantage of this huge strain recovery is to increase effective strain range, Figure 2.13. In contrast, normal material, such as stainless steel, when subjected to an excessive stress it would plastically deform and do not have an intrinsic recoverable strain, so the effective strain is not comparable with NiTi alloy, Figure 2.14.

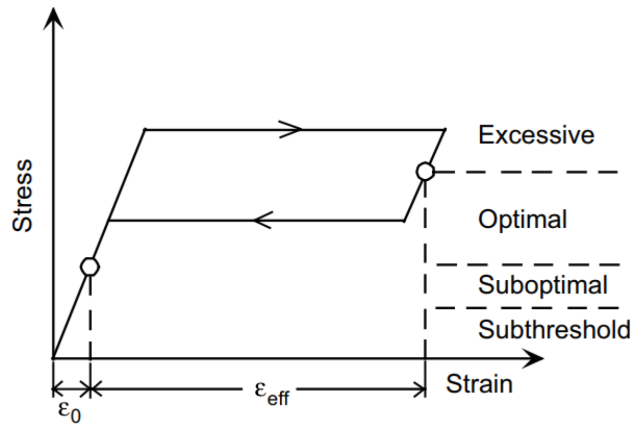

Figure 2.13 Stress-strain schematic diagram for Nitinol wire that exhibit superelasticity feature, and hence, the range of ε_{eff} is as larger as elastic wires [44].

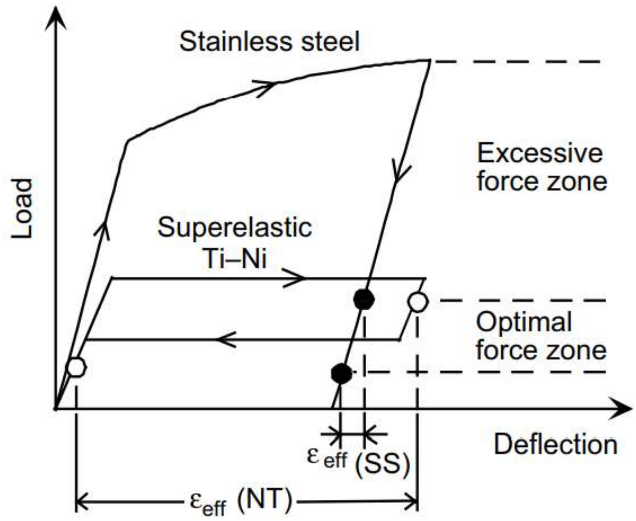

Figure 2.14 Load vs. deflection diagram for a stainless steel and NiTi orthodontic wires[44]. Stainless steel for increasing load more than yield point, and less than critical point, will plastically deform and cannot recover the force. But, since NiTi alloy due to martensitic transformation could save some energy in term of metastable martensitic phase, it could recover its prior morphology.

2.9.1.2 Spinal vertebral spacer

In human body spine is an essential organ that extended throw neck and bake which is includes 33 single vertebrate bones that are interlocked with each other and have intermediated tissue is called intervertebral disc. All together responsible to protect spinal cord, stand body, and give ability to human to bend and twist as well. All of them can got in problems, but intervertebral degenerate are most popular spinal problems which due to bad behavior can be happened and therefore mad back pain issue. Replacing them with some particular material can tackle the problem. One of the efficient candidates are SMAs, to create spinal spacer implant [45].

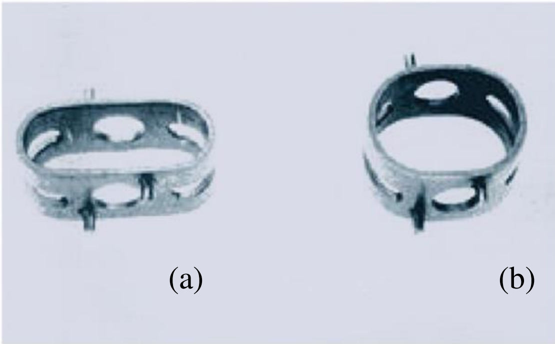

Figure 2.15 Spinal vertebral spacer were mad of SMA with (a) stable austenite, and (b) metastable martensite phase [12].

The pseudoelastic property of the SMAs is taken into account, which by using strain induced martensite tolerates an abnormal stretch and compression without losing its original shape. Thus, it does not restrict body's motions and prevent vertebrates to rub to each other [46].

2.9.1.3 Plates for fractured bone

Bon fracture can be healed under several conditions. One of the most important parameter is to make parts of fractured bones in contact. For this reason, special for facial bones, orthopedic surgeons implant some special plats and mini screws that are based on NiTi-SMA [47]. Nitinol has moderate stiffness could create a constant force. Also for each particular position the sample has to manufacture by laser welding.

Before it implanted in the fracture position, it has to manually get a small deformation, and thus the plate used its pseudoelasticity and hence create a constant force that is help to healing bones in a short time Figure 2.16.

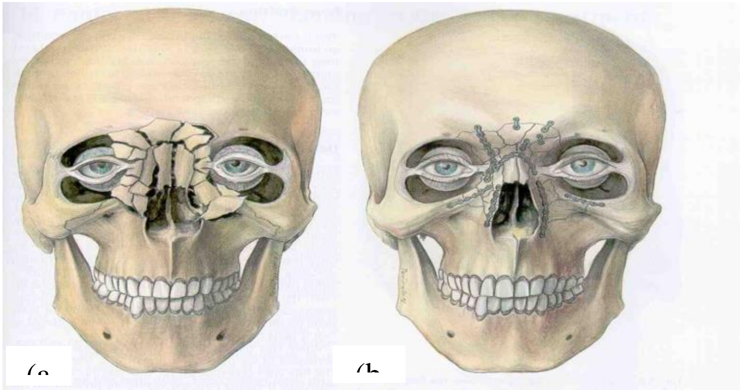

Figure 2.16 (a) fracture bones in facial area. (b) Implanted SMA-based plates with mini screws to help fractured bones being in contact [44].

2.9.2 Industrial Uses

Thermovariable rate spring, TVR spring, are made of Ni-Ti alloy that its size could be controlled. TVR are formed in its austenite phase, so if under a mechanical load it deformed in its martensitic phase it will re-morph by heating method. One of its application could be mentioned a sensor that is responsible to control switching of RPM transmission, Figure 2.17. In this case with a steel biasing spring embedded in a valve that is smaller than the total length of both springs. In a normal condition the steel spring compresses the TRV spring and pushed an intermediate piston to close the valve. However when the temperature of transmission increased to some particular degree the Ni-Ti spring activated by changing its phase and thus due to this transformation it could induced a force that could conversely pushed the piston and opens the gate to follow the transmission fluid. It could increase the efficiency of engine and reduce the smog produced and fuel exhausting [48].

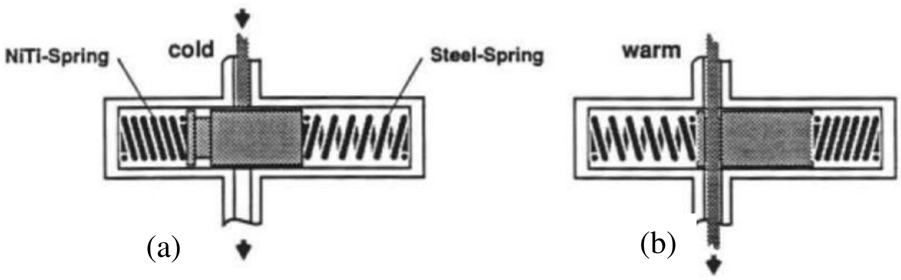

Figure 2.17 Two modes of thermostatic controlling valve in (a) close, and (b) open [48].

In sure, there are a lot of applications that are based on Ni-Ti SMAs because of its interesting feature. Describing all manufacturing apparatuses is beyond of this report. So briefly some of them are mentioned as follows:

i. For controlling temperature as actuator.
ii. These metals are often utilized in some watch springs, which are worked mechanically.
iii. It some microphones and to give a flexibility intelligent smartphones.

2.10 Addition of other element in NiTi

SMAs based on nickel and titanium has to data provided the best combination of material properties for most commercial use. Ni-Ti binary system of SMAs possess high ductility, excellent corrosion resistance in various environment including body fluids, despite all these properties the commercial application are limited due to expensive cost and complexity of production.

Ti-Ni thin films, fibers, particles and porous bulks have been successfully fabricated in recent years , and these materials, either in the monolithic form or in combination with other materials, have exhibited some exciting application potentials in microelectronic mechanical systems, medical implants, intelligent materials and structural systems in binary alloys, impact of Alloy Elements in the Ni-Ti system The binary standard Ni-Ti-based alloys deliver quite convenient properties in the transformation temperatures range between-30 and +80 ^{o}C. They exhibit superelasticity and shape memory behavior, combined with an excellent biocompatibility (in the case of proper treated surfaces nil but also good enough in normal conditions, even if sometimes dis- cussed controversy (12)) and are therefore successfully applied for orthodontic devices and other medical applications (3, 12) Besides this, other applications require transformation temperatures beyond those of the binary system (e.g. Sensors), or a wider or narrower hysteresis (e.g. Actuators) this can be attained by the addition of third and fourth elements to the binary alloy system. The addition of third or fourth elements to Ni-Ti-based alloys provides a powerful tool for controlling the properties and can be used to:

- control transformation temperatures
- increase the stability of Ms with respect to thermal history
- control the hysteresis width
- increase austenite strength
- reduce or increase martensitic strength
- increase two-way effect ability

High temperature transformation the basis of many investigations in recent times [13-20] ternary alloy systems like (Ni Ti-Pd), (Ni-Ti-Pt), (Ni-Ti-Hf), (Ni-Ti-Zr), and (Ni-Ti-Al), have been studied to explore their properties, including engineering considerations like manufacturing, phase stability, mechanical stability, and cost.

2.11 Instruments in use

2.11.1 Differential scanning calorimetry (DSC)

Differential scanning calorimetry, DSC, is a powerful technique in which the changes in heat capacity of materials can be measured. The heat capacities of materials is a function of temperature, whereby, through cooling or heating process its value changes. This device is the most common thermal analysis technique and is found in many analytical, process control, quality assurance and R&D laboratories, and it has a widely application in the field of pharmaceuticals, polymers, nanomaterial, and food products. In general, DSC is classified into two types according to the sample heating process, including power- compensation and heat flux DSC. In the first type, the temperature of both sample and reference are controlled individually by utilizing separate heating sources (furnaces). In this process, both sample and reference are supposed to have the same temperature, or coaxing together by varying the input powers of furnaces. The required power to do this is a measure of the change of enthalpy or heat capacity in the sample relative to the reference.

However, the heating source of the sample and the reference is the same source by using only one furnace in heat flux DSC type. The sample and the reference are connected to each other through a metal disc, the disc has a very low resistance heat flow path in which allowed the sample and the reference to have very good heat contact. Therefore, the heat flow is small compared with that in differential thermal analysis (DTA), and the changes in thermodynamics parameter that accompanies with temperature variation are recorded accurately.

Figure 2.18 shows the schematic diagram of DSC, and a DSC that monitored by a computer.

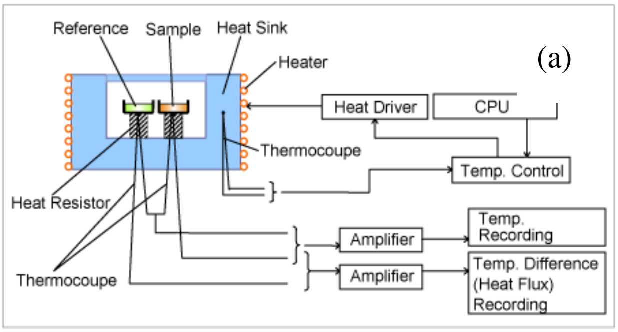

Figure 2.18 (a) schematic diagram of DSC device with sample and reference position, and electronic system. (b) DSC with computer monitoring.

2.11.2 Thermogravimetric Analysis (TGA)

Thermogravimetric Analysis (TGA) can be defined as a technique, whereby the mass of a given sample is measured as a function of temperature and time, thus during heating process the mass of substance either increase (oxidation) or decrease (evaporation) through a controlled environment. The TGA, in general, consists of a pan that holds the sample, sublimated by a precision balance. Then, the sample is heated or cooled in a furnace through placing the pan in. The mass of the sample is monitored during the experiment. A sample purge gas controls the sample environment. This gas may be inert (e.g. argon) or a reactive gas (e.g. oxygen) that flows over the sample and exits through an exhaust.

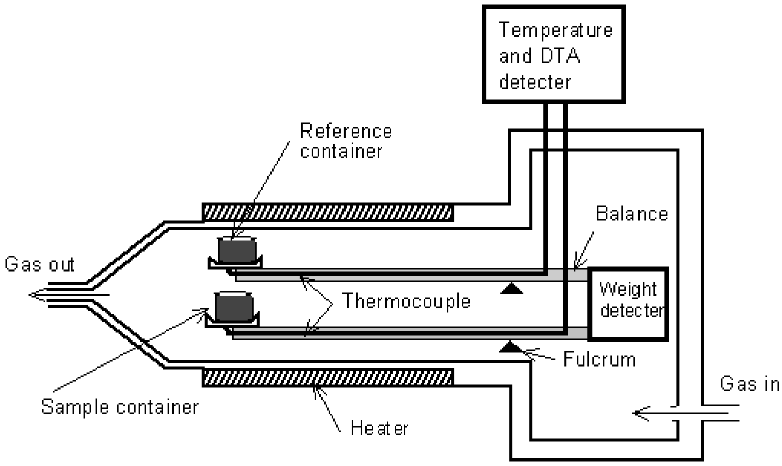

Figure 2.19 Schematic diagram of TGA system with reference container, sample container, weight detector, thermometer, and atmospheric control system [2, 49].

2.11.3 Arc-melter

Electric arc furnaces are the main means of recycling steel scrap and converting it to molten steel and is currently being used in molten steel production Fe ores. Such as direct reduction iron (DRI), Fe pig and molten steel, in a very high temperature furnace. Each shipment is called "pouring" range. For the production of shipments of special steel and the process of casting in the crucible. For each process, first the chamber of arc-melter vacuumed, and then an inert gas (argon) will injected into it, which do not interact with samples. Then by using a special electrode the target sample will melted. After that, the toxic gas of chamber should be pumped to outside and then it fills with natural gas. Normally, the sample cooled down naturally.

The charge used in the electric arc furnace includes the following raw materials:

- Hard scrap
- Fused steel
- Iron produced by direct reduction.

Figure 2.20 Arc-melter for preparing metallic alloy with atmosphere control system.

2.11.4 X-ray diffractometer (XRD)

X- ray diffractometer (XRD), is a characteristic tool that have been used to study the structure of materials by projecting a beam of the x-ray to the surface of a given sample from different angle of incidence of the x-ray beam. During the process, the x-ray beam will scatter and interact with atoms or molecules of the given sample. Then by measuring incident angle and diffracted x-ray from the sample, an accurate pattern will obtained, which includes information about crystallography of the sample. Moreover, the important physical parameters such as precision, speed of rotations and beam size of x-ray have a crucial influences on the results.

XRD can used for analyzing a wide range of materials, including fluids, metals, minerals, polymers, catalysts, plastics, pharmaceuticals, thin- film coatings, ceramics, solar cells, and semiconductors. In addition, XRD has become an indispensable method for materials investigation, characterization and quality control. Example areas of application include qualitative and quantitative phase analysis, crystallography, structure and relaxation determination, texture and residual stress investigations [50].

By using XRD pattern, one can calculated lots of parameters, including lattice parameter, different phase in the sample, grain size, and so on [51, 52].

Figure 2.21 X-ray diffraction device for crystallography.

2.11.5 SEM-EDX

Energy Dispersive X-ray Spectroscopy (EDX), is used to determine the composition of a sample such as shape memory alloys and thin films. EDX is an extension of the Sir ion Scanning Electron Microscope in the Molecular Analysis Facility.

In general, atoms are composed of nuclei (protons and neutrons) with electrons orbiting around them with different energy levels. When a high-energy electron beam from the SEM hit the sample, some of these electrons collide with electrons that occupied in the lower energy levels, then both of this electrons leave the atom. As a result, an electron located at a higher energy level jumps to the lower energy state. When the electron moves to this lower energy level, it releases energy – specifically, x-rays. Some of incident electron pass through a short distance of nuclei which due to coulombs attraction force they changed their direction, which produce another type of x-ray that known as characteristic x-ray. Also it is possible to have different x-ray with various wave lengths due to multiple electron transitions for an atom, because electrons can fall from different elevated levels.

The X-rays have a specific energy which is characteristic of the material and equal to the energy difference between excited and ground state electron orbitals in the atom.

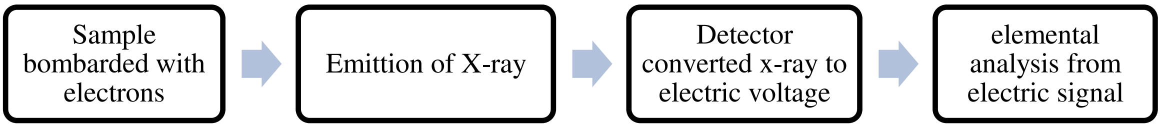

Figure 2.22 Scanning Electron Microscopy-Energy Dispersive X-ray Spectrometry (SEM-EDX).

2.11.6 Optical Microscope (OM)

Optical microscopy is an important tool that has been used to visually study surfaces of specimens (in range of micro-meter). It depends mainly on magnification lenses and visible lights, and it has widely application in many fields of science and industry like microelectronics, nano-science, biotechnology, material science, composite, alloys, pharmaceutical industry, and cell/microbiology. In addition, the images of the certain samples can be obtaining by using light sensitive cameras with optical microscopy. Recently, technological developments have enabled digital images to be taken with CMOS and charge-couple device (CCD) cameras for optical microscopes which can projected the images into computer's screen in a fraction of second with a high level of accurate.

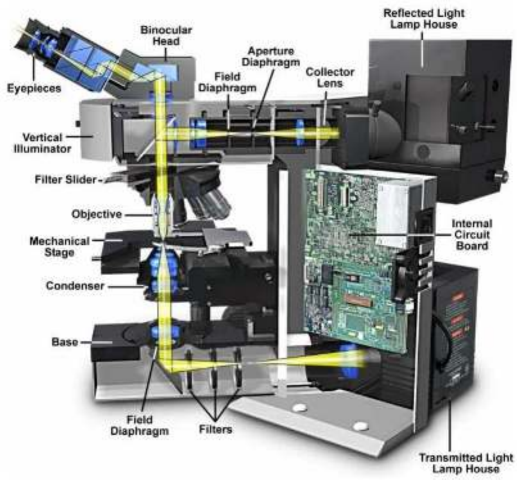

Figure 2.23 A modern optical microscope with an electronic board and other components [53].

3. EXPERIMENTAL PROCEDURE

3.1 Production

The atomic and mass % ratios of the main material NiTi and NiTi alloys with cobalt added are given in the Table 3.1. All of the produced alloys are coded with lettering. High purity (about % 99.9 purity) nickel, titanium and cobalt powders are homogenously mixed and powder mixtures are made into pellets. The mixture pellets were melted in the arc melting furnace under vacuum. When the alloy samples were in the arc furnace, the melting process was repeated several times and the primary homogenization process was carried out. The bulk samples removed from the furnace were kept at 1050 ^{o}C for 24 hours to increase homogeneity. The alloys which were kept for 24 hours were cooled from the furnace into salty ice water.

Table 3.1. Atomic values of predetermined composition of NiTiCo shape memory alloys and the general EDX results of NiTi and NiTiCo alloys after production.

	Production composition			Measured composition by EDX		
Alloy Code	**Ni (at. %)**	**Ti (at. %)**	**Co (at. %)**	**Ni (at. %)**	**Ti (at. %)**	**Co (at. %)**
Main NiTi (Co0)	49.0	51.0	------	49.08	50.92	------
Co2	46.5	51.5	2	46.59	51.15	2.26
Co3	45.0	52.0	3	45.09	51.91	3.00
Co4	43.5	52.5	4	42.71	53.11	4.18
Co5	42.0	53.0	5	41.79	53.08	5.13
Co6	40.5	53.5	6	39.61	54.00	6.31

3.2 Transformation temperature analysis via Differential Scanning Calorimetry

Differential scanning calorimetry (DSC) is a device commonly used to determine the phase transformation temperature of shape memory alloys.

The martensite ↔ austenite transformation temperatures of the NiTi and NiTiCo shape memory alloys were determined by DSC. Thermal analysis measurements were made at 10 ^{o}C /min. heating-cooling rate in an argon atmosphere.

3.3 Crystal structure analysis

X-ray diffraction methods are used to determine the exact dimensions of the unit cell in any crystal and to determine the structure of the atoms in the crystal structure. In this study, x-ray analyzes of the produced alloys were made by using Rigaku RadB-DMAX II computer controlled x-ray diffractometer by CuKα (λ = 1.5405Å) radiation. Measurements were made with a constant scanning speed of 6 ^{o}/min between 20^{o} and 80^{o}.

3.4 SEM-EDX analysis

SEM (Scanning Electron Microscopy) is an important device with multi-use which enables us to obtain information about the shape, size and arrangement of materials (morphology), determination of surface properties and structure of the material (topology), composition difference, crystal orientation and image of defects.

Electron microscopy images are taken from the outer surfaces of the alloys which are etched with Marble solution. Leo Evo-40xVP model electron microscopy was used for SEM analyzes.

3.5 Magnetization analysis

Magnetic measurements of the alloys were done at the room temperature with Quantum Design PPMS 7 (Physical Properties Measurement System) device, -5 Tesla and 5 Tesla magnetic fields range.

4. RESULTS AND DISCUSSIONS

The phase transformation between austenite and martensite phases was carried out by DSC measurement for all samples. By using peaks and trough appeared in exothermic and endothermic process some valuable information were achieved, including austenite start (A_s), austenite finish (A_f), martensite start (M_s), and martensite finish (M_f) temperatures. In addition, the change of internal energy was obtained by calculating the area under the peaks and troughs, which are known as enthalpy change. All of these aforementioned parameters have been listed in Table 4.1. Figure 4.1 specified that at room temperature each Co0, Co2, and Co3 are in austenite phase, and the others are in martensite phase. Also, martensitic transformation for all cases is occurred under room temperature. Moreover, samples with 2 and 3 Co-composition have a metastable phase, which is called R-phase, during cooling process. Thus, the austenite phase transferred from body centered cubic to rhombohedral (R) phase, then through dropping down temperature it finally reach martensite phase that its microstructure look like a zigzag form known as twin [54]. Also, R-phase was detected in Co4 for endothermic process, such as M→R→A, but Co5 and Co6 samples did not show R-phase during phase transformation process. It could be notice that adding more Co content led to disappear this intermediate phase.

The values of calculated enthalpy change are given in Table 4.1, and they illustrated in Figure 4.2. It is obviously can be seen the ΔH increased for alloys that in RT have austenite phase, while for the others its value suddenly mitigated.

Table 4.1 DSC measurement results of the alloys.

Alloy Code	A_s (K)	A_f (K)	M_s (K)	M_f (K)	$\Delta H_{M\to A}$ *kJ/kg*	$\Delta H_{A\to M}$ *kJ/kg*	$\Delta S^{A\to M}$ (J/kg K)	$\Delta S^{M\to A}$ (J/kg K)
Main NiTi (Co0)	303	325	279	244	5.39	2.69	8.91	17.86
Co2	300	332	291	251	7.35	0.8	2.70	24.79
Co3	298	331	295	238	9.66	1.4	4.74	32.73
Co4	295	308	281	266	3.15	0.57	1.94	10.70
Co5	279	295	269	264	1.7	1.21	4.29	6.03
Co6	263	279	253	244	1.07	0.72	2.70	4.02

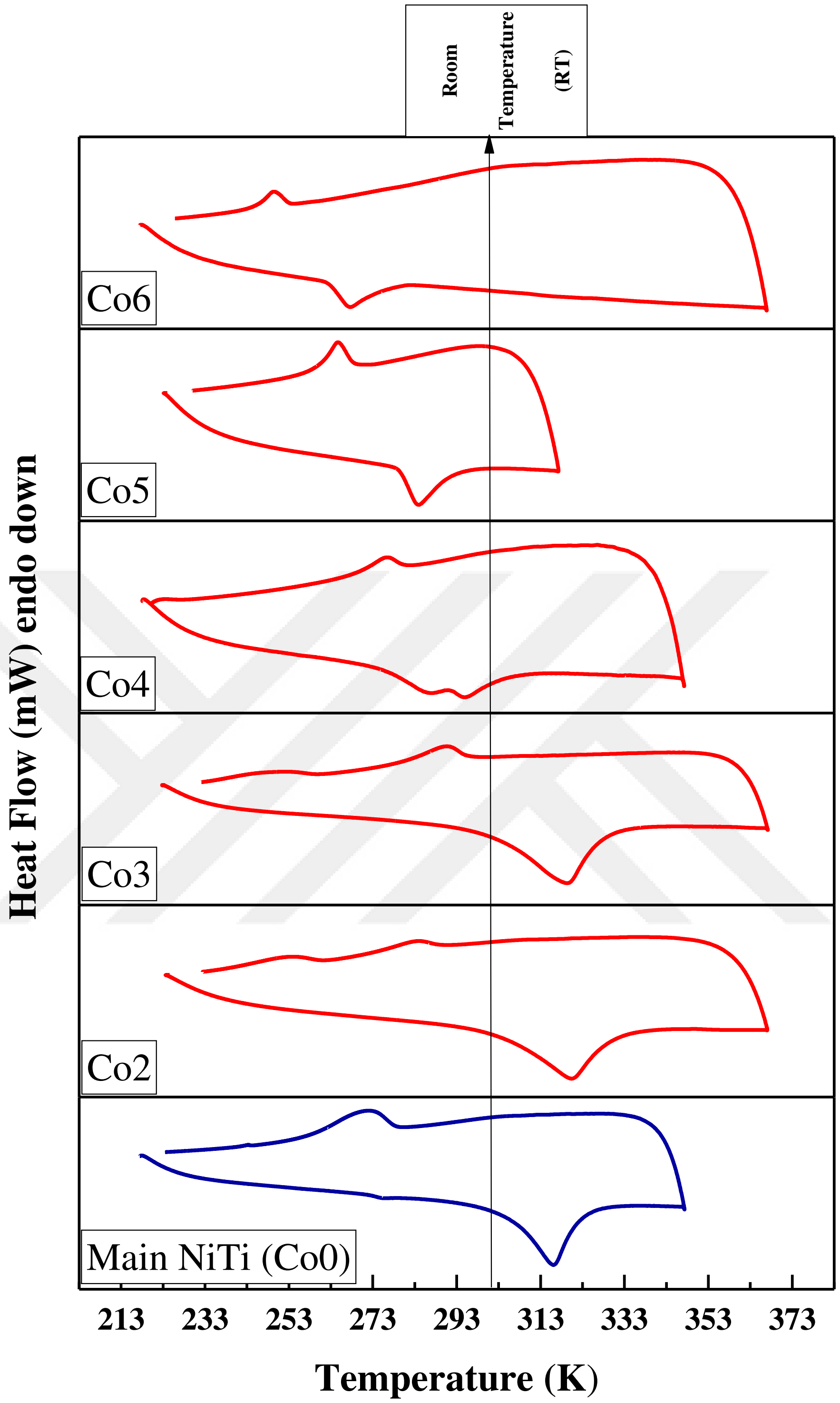

Figure 4.1 Phase transformation curves of samples.

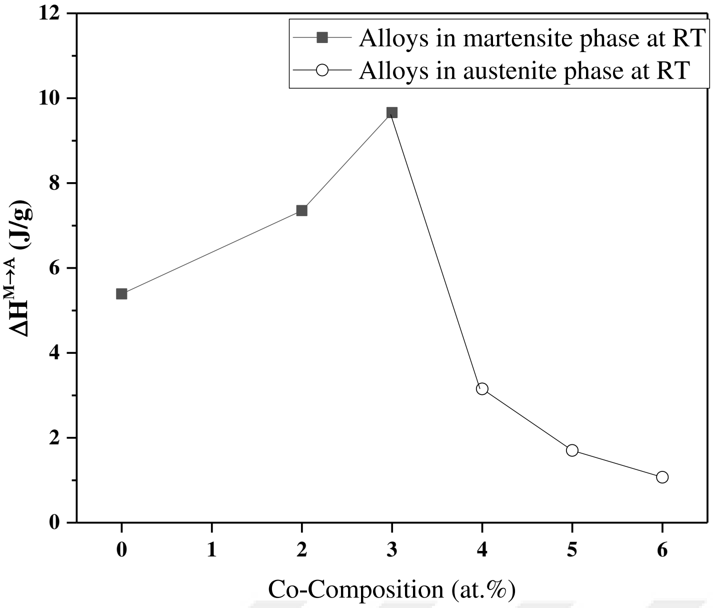

Figure 4.2 Enthalpy change values for austenite phase transformation of all alloys.

Since, there is a close relationship between some physical quantities, and then it is convenient to introduce the derivative mathematical formulas to calculate Gibbs free energy (ΔG) and some related thermodynamics values. To begin with, equivalent temperature (T_o) is point where ΔG for austenite ↔ martensite transformation is equal to zero, and represented as [2, 55]:

$$T_o = \frac{1}{2}\left(M_s + A_f\right) \tag{4.1}$$

By extending this assumption, Gibbs free energy for an endothermic process could be given as [56]:

$$\Delta G^{M\to A} = G^A(T_o) - G^M(T_o) = (H^A - T_o S^A) - (H^M - T_o S^M)$$
$$= \Delta H^{M\to A} - T_o \Delta S^{M\to A} = 0 \tag{4.2}$$

where, G, H, and S are Gibbs free energy, enthalpy and entropy of the alloy, respectively. Also the superscript *M* and *A* are referred martensite and austenite phases. The mathematical relation between each equilibrium temperature, enthalpy and entropy changes can be expressed as the following equation:

$$T_o = \frac{\Delta H^{A\to M}}{\Delta S^{A\to M}} = \frac{\Delta H^{M\to A}}{\Delta S^{M\to A}}. \tag{4.3}$$

By using achieved values of enthalpy that is given in Table 4.1 and handling Eq. (4.3), for each specimen, change of entropy could be obtained. The obtained results compared with each other and illustrated in Figure 4.3. There is a dramatic increase in the value of $\Delta S^{A\to M}$for Co0, Co2, and Co3 alloys, and then it significantly decreased for the rest of alloys.

Since, there is a straight relationship between enthalpy and entropy change of alloys, then the value $\Delta S^{A\to M}$ depends on the value of $\Delta H^{A\to M}$. Once more, the variation in the different results is due to the different in type of phases. In exothermic process, this difference cannot obviously see.

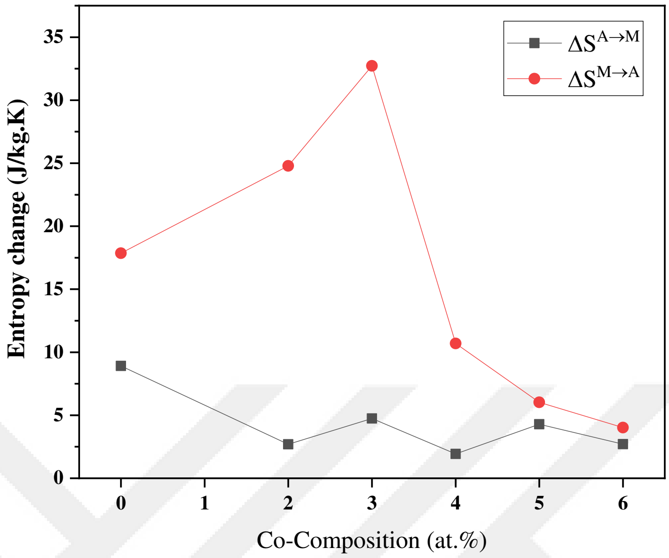

Figure 4.3. Entropy change of both endothermic and endothermic process for all samples.

Both the force for nucleation and the temperature hysteresis in a SMAare important parameters, but first of all the Gibbs free energy through exothermic process should be calculated as follows:

$$\Delta G^{A\to M}(M_s) = \Delta G^{M\to A}(T_o) - \Delta G^{M\to A}(M_s) = -(T_o - M_s)\Delta S^{M\to A} \quad (4.4)$$

When a force applied to an object, it will saved as a potential energy in the stretched crystal, and due to unloaded process the elastic object give back stored energy and return back to its pre-morphology. This energy, which is called elastic energy (G_e), in SMAs appears inside martensite variants. The Gibbs free energy needed in an endothermic process, and the subtraction between M_s and A_f, are the only values to find out G_e [56]:

$$G_e = \Delta G^{A\to M}(M_s) - \Delta G^{A\to M}(M_f) = (M_s - M_f)\Delta S^{M\to A} \quad (4.5)$$

Figure 4.4 illustrates the effect of cobalt composition on G_e and $\Delta G^{A\to M}$. While, increasing Co led to continuous decrease in G_e, the Gibbs free energy has two different situation. First ΔG increased for those samples that showed martensite phase in room temperature. The second portion showed the samples with austenite phase in room temperature, where increasing cobalt causes ΔG decreased.

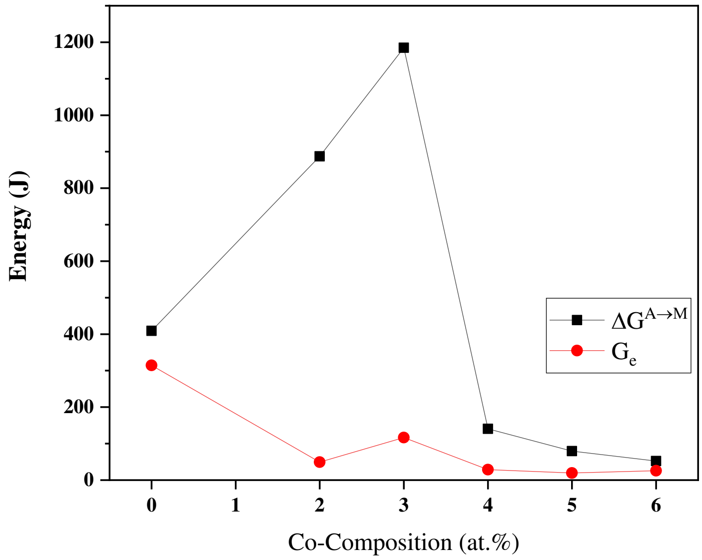

Figure 4.4 Change of Gibbs free energy during martensite phase transformation and elastic energy for different Co-composition rates.

To show up the existing of different phases in each samples, XRD measurement with scanning speed of 6 °/min accomplished at room temperature. The XRD outcomes for Co0, Co2, and Co3 displayed in Figure 4.5a, and likewise, these results for Co4, Co5, and Co6 is shown in Figure 4.5b. All determination phases has been checked out by JCPDS cards (cards no:18-0898,65-5746,65-4572) and existing literature [57-60]. Ti_2Ni phase, which has face centered cubic crystal structure, is appeared in all alloys [61]. All Co0, Co2, and Co3 samples showed B19′- martensitic phase. This phase has monoclinic crystal structure, which is normally can make twins and zigzag-like structure. Increasing Co-addition led to disappeared martensite peaks in the range of 39 ^{o} to 40^{o}. In the Figure 4.5b, the most extensive phase is B2 phase with Ti2Ni is found to be second precipitation phase in each Co4, Co5, and Co6 alloys. B2 phase with high similarity has body centered cubic crystal structure [61]. In the inset of Figure 4.5b is can be determine that Co4 alloy has a sharp XRD peak and increasing Co composition to 5 and 6 at.% causes to split these peaks.

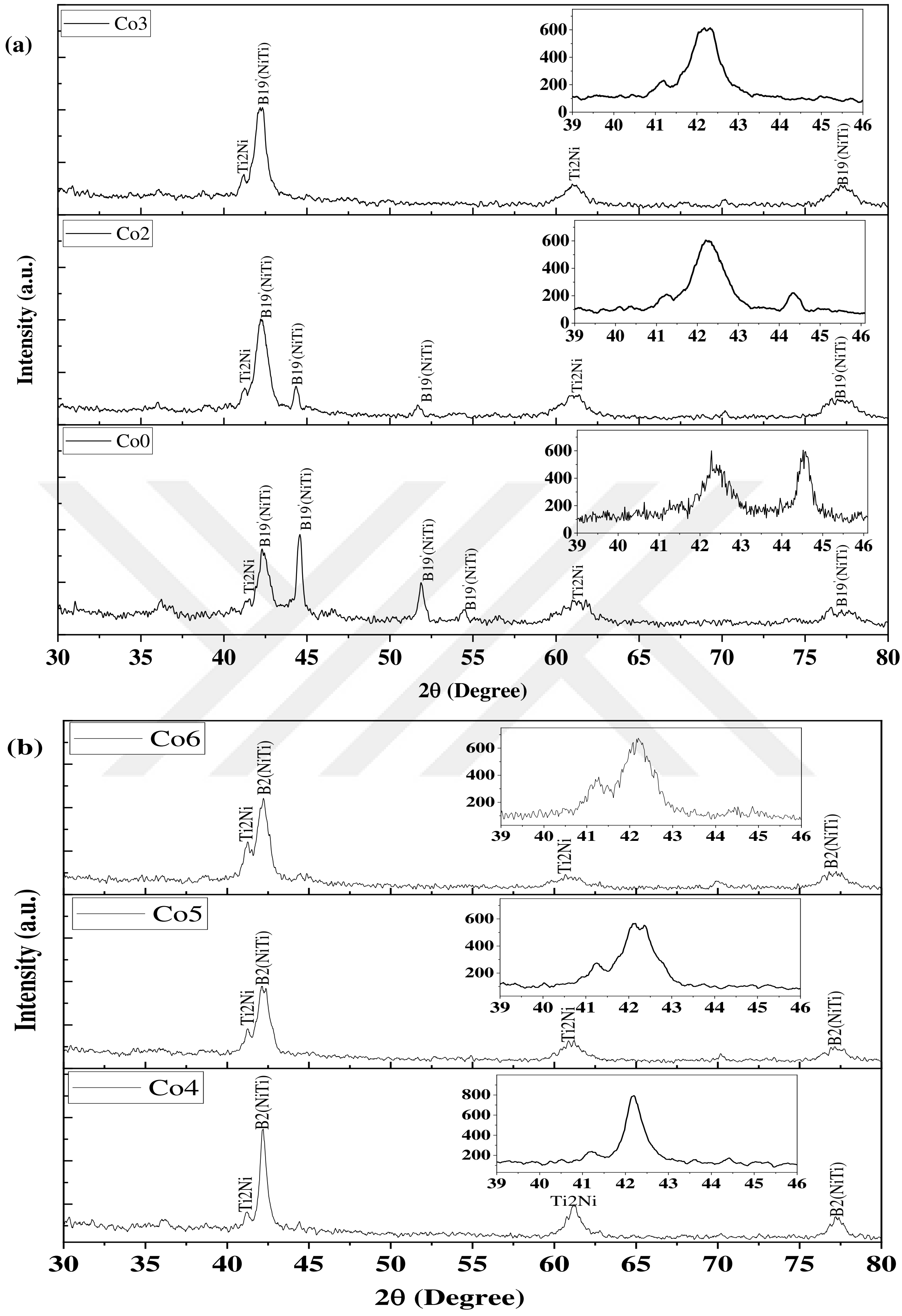

Figure 4.5 XRD diffractograms of main NiTi (Co0) and NiTiCo (with cobalt amount of 2, 3, 4, 5, and 6 at. %) shape memory alloys. (a) The samples that situated in austenite phase at RT

and (b) samples with cobalt composition of 4, 5, and 6 at. % shows martensite phase in RT. The insets showed sharpest peak in x-ray diffractograms clearly.

For all samples SEM images are shown in Figure 4.6, and EDX measurement has performed for determining chemical compositions of some points and region, where the results given in Table 4.2. The dominant phase for each Co0, Co2, and Co3 alloys are B19′ (NiTi).

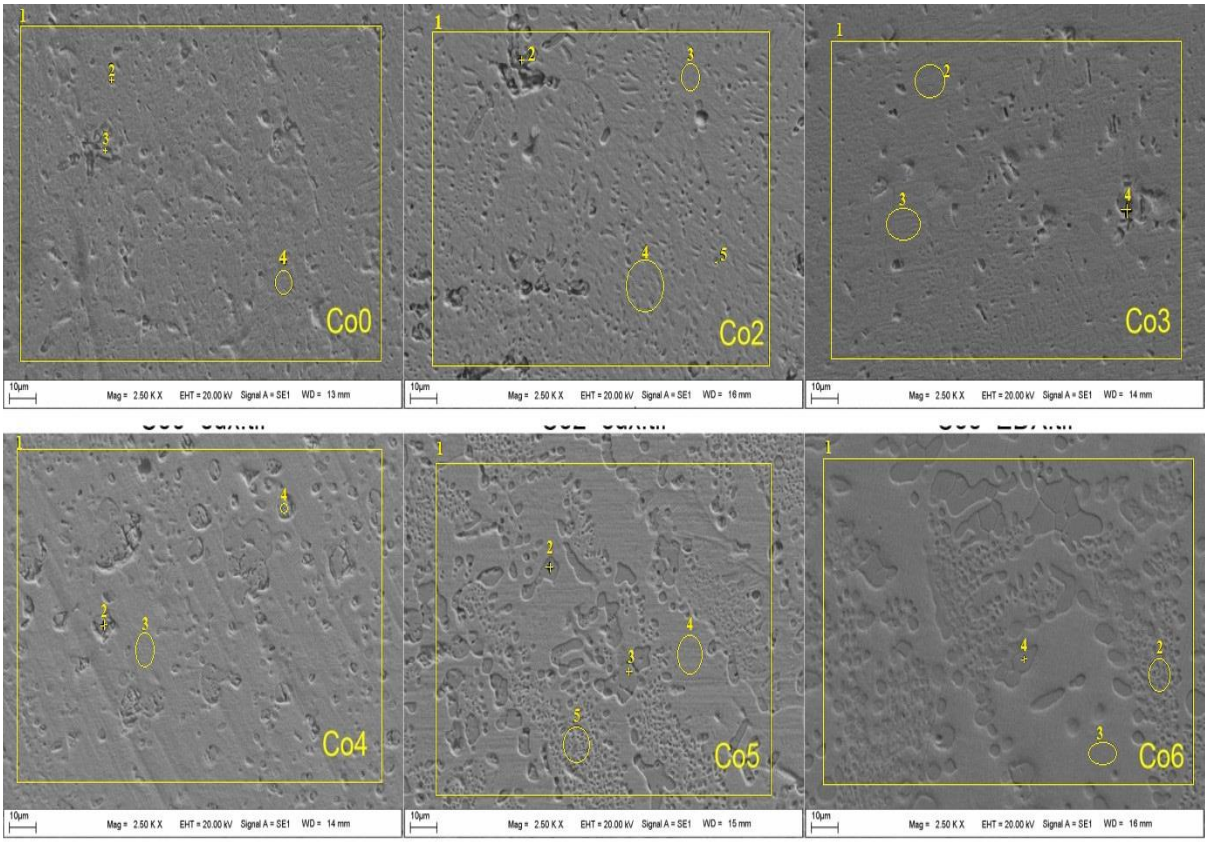

Figure 4.6 SEM images of NiTi and NiTiCo shape memory alloys with labeled some position of EDX measurements.

Also Ti2Ni are the second phase is specified for mentioned alloys. On the other hand, the EDX measurements for Co4, Co5, and Co6 illustrated that the matrix of these alloys are austenite and has B2 (NiTi) phase. The second phase, existing as precipitations, were Ti2Ni phase, which its amount increased with increasing Co rate. As Yi, H. C [62] and X.J. Yan [63] reported, in NiTi SEM images some dendritic phase appeared, where the growth of them are in the same direction that the NiTi alloys has cooled down. It is found that the amount dendritic phase (Ti2Ni) enhanced with increasing Co additive. Phase determination by only chemical composition achieved from EDX is difficult because the atomic mass percentage of

Ni and Ti approximately the same in the alloys. Thus, martensite and austenite phases were specified by SEM images, and then some specific positions measured by EDX. The result showed that Ti2Ni phase contained 30% Ni and 60% Ti. In addition, this phase is exist in either martensite or austenite [61, 64].

Table 4.2 Chemical composition results of NiTi and NiTiCo alloys in different region on SEM images.

Alloys code	Spectrum no	Ni (%at.)	Ti (%at.)	Co (%at.)	Phases
Co0	**1**	50.92	49.08	-----	B19′
	2	49.76	50.24	-----	B19′
	3	30.59	69.41	-----	Ti_2Ni
	4	49.87	50.13	-----	B19′
Co2	**1**	46.59	51.15	2.26	B19′
	2	30.83	67.84	1.33	Ti_2Ni
	3	47.75	50.01	2.24	B19′
	4	46.18	51.46	2.47	B19′
	5	33.29	65.39	1.31	Ti_2Ni
Co3	**1**	45.09	51.91	3.00	B19′
	2	46.38	50.39	3.23	B19′
	3	45.22	51.69	3.09	B19′
	4	32.93	65.34	1.74	Ti_2Ni
Co4	**1**	42.71	53.11	4.18	B2
	2	30.94	66.64	2.42	Ti_2Ni
	3	44.72	50.64	4.64	B2
	4	32.16	64.94	2.90	Ti_2Ni
Co5	**1**	41.79	53.08	5.13	B2
	2	30.93	65.76	3.31	Ti_2Ni
	3	30.22	66.95	2.84	Ti_2Ni
	4	43.95	50.63	5.42	B2
	5	42.39	52.63	4.98	B2
Co6	**1**	34.61	54.08	6.31	B2
	2	39.68	54.44	5.88	B2
	3	42.49	50.59	6.92	B2
	4	29.00	67.08	3.92	Ti_2Ni

Figure 4.7 illustrated OM images in scale of 250 µm. Co alloy showed martensite plates, and among them some star-shaped dendrites appeared. Likewise, both Co2 and Co3 displayed martensite plates in their OM images. The star-shaped dendrites transferred their shape to rods-shapes when cobalt composition increased to 4 and 6 at.%, while there is no martensite plates could be found in them [65]. Moreover, in Co6 alloy some precipitation phases formed.

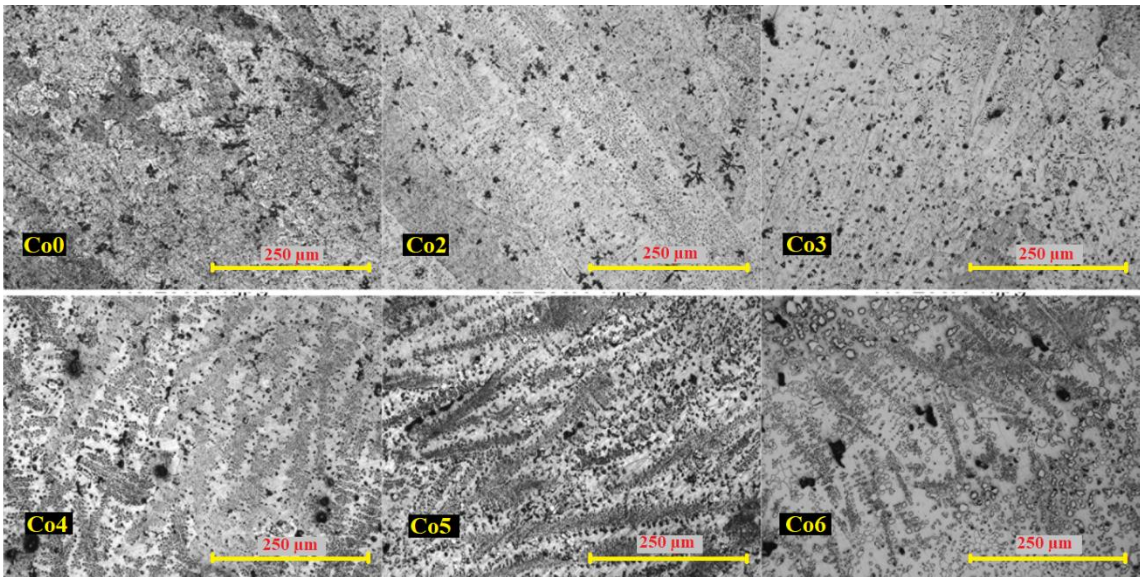

Figure 4.7 Optical microscopy images of NiTi and NiTiCo alloys at room temperature.

For all specimens in room temperature with a high optical microscope were prepared.

To investigate the magnetic property of all samples, the magnetization measurements were performed and the results shown in Figure 4.8. The magnetization results for those alloys that showed austenite in room temperature were less than the other cases. There are a few studies measured magnetization of NiTi-based alloys, such as Gururaja et al. [66], that conducted a study based on both theory and experiment, for magnetic property of Fe-doped NiTi alloy. Thus, this measurement could be the important and a rare part in this study, especially the main differences in magnetization of martensite and austenite phases.

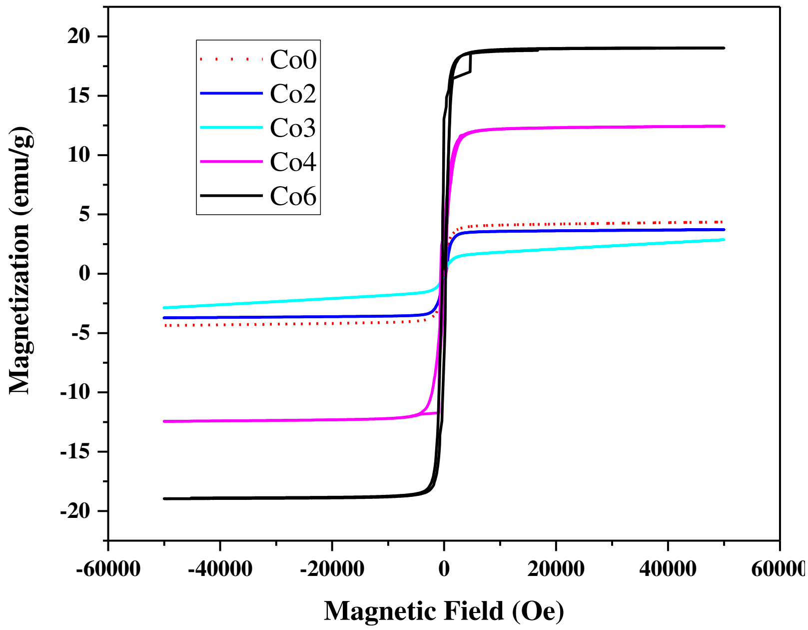

Figure 4.8 Magnetization curves of Co0, Co2, Co3, Co4 and Co6 alloys at RT.

The magnetic coercivity of Co0, Co2, Co3, Co4 and Co6 alloys are displayed in Figure 4.9. Since, both nickel and cobalt are ferromagnetic materials, then all alloys be magnetize even after the external magnetic field disappeared [67]. The quantitative value of magnetic field needed to reduce the stored magnetization in these alloy is known as coercivity. The value of coercivity by increasing from Co0 to Co3 decreased, but in Co4 and Co6 the value dramatically increased. The difference in phases could be the only reason that effected on values of coercivity.

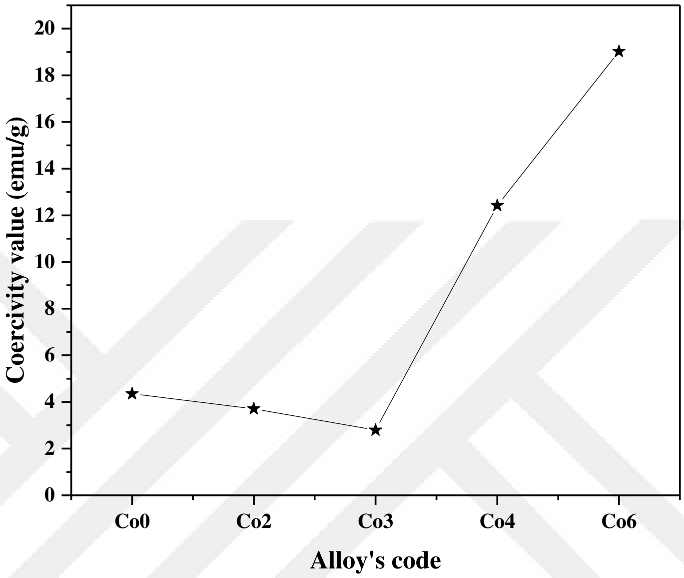

Figure 4.9 Coercivity values of Co0, Co2, Co3, Co4 and Co6 shape memory alloys.

5. CONCLUSION

In this study the influence of additional Co-composition on NiTi shape memory alloy investigated from different perspectives. To conclude, the important results summarized in following built points:

Thermal Analysis:

- At room temperature each Co4, Co5, and Co6 alloys had austenite phase, while Co2, Co3, and main alloy had martensite phase.
- In general, all both austenite start and martensite start temperature decreased by adding Co additive to the NiTi alloy.
- The enthalpy change value depended on the status of crystal structure, whereby, increasing Co additive led to increase ΔH values for those alloys that showed austenite phase in room temperature, while ΔH values decreased with increasing Co-content in the alloys that found to have martensite phase in room temperature.
- Since, both enthalpy and entropy has close relationship, then its value for martensite transformation first increased for Co0, Co2, and Co3 alloys, and for Co4, Co5, and Co6 alloys its value decreased. For austenite phase transformation by increasing cobalt additive to NiTi alloy, ΔS value fluctuated approximately between 7.5-2.5 (J/kg.K).

Crystal and Microstructural Analysis:

- According to XRD results which were taken at room temperature, Co0, Co2 and Co3 have two phases: one of them Ti2Ni precipitate phases, other is B19′ martensite phase. Co4, Co5 and Co6 showed that Ti2Ni precipitate phase and austenite phase.
- SEM-EDX results were supported by XRD data. It can be seen that two phases chemical compounds and microstructural properties all of alloys.
- From different measurement and observations, such as XRD, SEM-EDX, and optical microscopy, it is found that all alloys have Ti2Ni phase, also, after Co composition exceed, from Co4 to Co6 the austenite finish temperature dropped to less than room temperature.

Magnetization Analysis:

- Even the magnetization measurements showed that there are different in those alloys that have martensite or austenite during carried out measurement at room temperature. The results showed that austenite phase alloys has a higher magnetization saturation compared to the other with martensite phase.
- The coercivity value decreased from Co2 to Co3, but the value was significantly increased in Co4 and Co6. The difference in the stages can be the only reason that affects the values of coercivity.

REFERENCES

[1] **Kök, M., Zardawi, H.S.A., Qader, I.N., and Kanca, S.**, 2019. The Effects of Cobalt Elements Addition on Ti2Ni Phases, Thermodynamics Paramaters, Crystal Structure and Transformation Temperature of NiTi Shape Memory Alloys *The European Physical Journal Plus*.

[2] **Qader, I.N., Kök, M., and Dağdelen, F.**, 2019. Effect of heat treatment on thermodynamics parameters, crystal and microstructure of (Cu-Al-Ni-Hf) shape memory alloy, *Physica B: Condensed Matter*, **553**, 1-5.

[3] **Dağdelen, F., Aldalawi, M.A.K., Kök, M., and Qader, I.N.**, 2019. Influence of Ni addition and heat treatment on phase transformation temperatures and microstructures of a ternary CuAlCr alloy, *The European Physical Journal Plus*, **134**(66).

[4] **Khalil-Allafi, J., Dlouhy, A., and Eggeler, G.**, 2002. Ni4Ti3-precipitation during aging of NiTi shape memory alloys and its influence on martensitic phase transformations, *Acta Materialia*, **50**(17), 4255-4274.

[5] **Stroz, D., Kwarciak, J., and Morawiec, H.**, 1988. Effect of ageing on martensitic transformation in NiTi shape memory alloy, *Journal of Materials Science*, **23**(11), 4127-4131.

[6] **Otubo, J., Rigo, O., Coelho, A., Neto, C.M., and Mei, P.**, 2008. The influence of carbon and oxygen content on the martensitic transformation temperatures and enthalpies of NiTi shape memory alloy, *Materials Science and Engineering: A*, **481**, 639-642.

[7] **Kök, M., Aydoğdu, Y., Dağdelen, F., and Ateş, G.**, 2017. Improving of the surface properties of NiTiCu shape memory alloy by oxidation NiTiCu şekil hatırlamalı alaşımın oksidasyon ile yüzey özelliklerinin geliştirilmesi, *Dicle University Institute of Natural and Applied Science Journal*, 1-5.

[8] **Gong, C., Wang, Y., and Yang, D.**, 2006. Martensitic transformation of Ni50Ti45Ta5 shape memory alloy, *Journal of Alloys and Compounds*, **419**(1-2), 61-65.

[9] **Ölander, A.**, 1932. An electrochemical investigation of solid cadmium-gold alloys, *Journal of the American Chemical Society*, **54**(10), 3819-3833.

[10] **Greninger, A.B. and Mooradian, V.G.**, 1938. Strain transformation in metastable beta copper-zinc and beta copper-Ti alloys, *AIME TRANS*, **128**, 337-369.

[11] **Kauffman, G.B. and Mayo, I.**, 1997. The story of nitinol: the serendipitous discovery of the memory metal and its applications, *The chemical educator*, **2**(2), 1-21.

[12] **Buehler, W.J., Gilfrich, J., and Wiley, R.**, 1963. Effect of low- temperature phase changes on the mechanical properties of alloys near composition TiNi, *Journal of applied physics*, **34**(5), 1475-1477.

[13] **Buehler, W.J. and Wang, F.E.**, 1968. A summary of recent research on the Nitinol alloys and their potential application in ocean engineering, *Ocean Engineering*, **1**(1), 105-120.

[14] **Hartl, D., Lagoudas, D., Calkins, F., and Mabe, J.**, 2009. Use of a Ni60Ti shape memory alloy for active jet engine chevron application: I. Thermomechanical characterization, *Smart Materials and Structures*, **19**(1), 015020.

[15] **Petrini, L. and Migliavacca, F.**, 2011. Biomedical applications of shape memory alloys, *Journal of Metallurgy*, **2011**.

[16] **Duerig, T.W., Melton, K., and Stöckel, D.**, 2013. Engineering aspects of shape memory alloys, Butterworth-Heinemann.

[17] **Wang, F.E. and Buehler, W.J.**, 1972. Additional unique property changes observed during TiNi transition, *Applied Physics Letters*, **21**(3), 105-106.

[18] **Sun, L. and Huang, W.**, 2009. Nature of the multistage transformation in shape memory alloys upon heating, *Metal Science and Heat Treatment*, **51**(11), 573-578.

[19] **Mihálcz, I.**, 2001. Fundamental characteristics and design method for nickel-titanium shape memory alloy, *Periodica Polytechnica. Engineering. Mechanical Engineering*, **45**(1), 75.

[20] **Zanaboni, E.**, 2008. One Way and Two Way-Shape Memory Effect: Thermo-Mechanical Characterization of Ni-Ti Wires, *Universita degli Studi di Pavia, Pavia, Italy*.

[21] **Huang, H.L., Park, S.-H., Park, J.-O., and Yun, C.-H.** *Development of stem structure for flower robot using SMA actuators*. in *Robotics and Biomimetics, 2007. ROBIO 2007. IEEE International Conference on*. 2007. IEEE.

[22] **Park, H., Jung, S., Choi, J., Park, S., Yoon, C., and Park, J.** *A study on the moving mechanism for flower robot*. in *Control, Automation and Systems, 2007. ICCAS'07. International Conference on*. 2007. IEEE.

[23] **Tao, T., Liang, Y.-C., and Taya, M.**, 2006. Bio-inspired actuating system for swimming using shape memory alloy composites, *International Journal of Automation and Computing*, **3**(4), 366-373.

[24] **Liang, Y., Kuga, Y., and Taya, M.** *Design of synthetic jet actuator based on FSMA composite*. in *Smart Structures and Materials 2005: Industrial and Commercial Applications of Smart Structures Technologies*. 2005. International Society for Optics and Photonics.

[25] **Nishida, M., Tanaka, K., and Wang, H.O.** *Development and control of a micro biped walking robot using shape memory alloys*. in *Robotics and Automation, 2006. ICRA 2006. Proceedings 2006 IEEE International Conference on*. 2006. IEEE.

[26] **Reynaerts, D., Peirs, J., and Van Brussel, H.**, 1999. Shape memory micro-actuation for a gastro-intestinal intervention system, *Sensors and Actuators A: physical*, **77**(2), 157-166.

[27] **Menciassi, A., Gorini, S., Pernorio, G., and Dario, P.** *A SMA actuated artificial earthworm*. in *Robotics and Automation, 2004. Proceedings. ICRA'04. 2004 IEEE International Conference on*. 2004. IEEE.

[28] **Chu, W.-S., Lee, K.-T., Song, S.-H., Han, M.-W., Lee, J.-Y., Kim, H.-S., Kim, M.-S., Park, Y.-J., Cho, K.-J., and Ahn, S.-H.**, 2012. Review of biomimetic underwater robots using smart actuators, *International journal of precision engineering and manufacturing*, **13**(7), 1281-1292.

[29] **DeLaurentis, K., Mavroidis, C., and Pfeiffer, C.** *Development of a shape memory alloy actuated robotic hand*. in *7th International Conference on New Actuators (ACTUATOR 2000), Bremen, Germany, June*. 2000.

[30] **Laurentis, K.J.D. and Mavroidis, C.**, 2002. Mechanical design of a shape memory alloy actuated prosthetic hand, *Technology and Health Care*, **10**(2), 91-106.

[31] **Hino, T. and Maeno, T.** *Development of a miniature robot finger with a variable stiffness mechanism using shape memory alloy*. in *International Symposium on Robotics and Automation, Querétaro, México, Aug*. 2004.

[32] **Maeno, T. and Hino, T.** *Miniature five-fingered robot hand driven by shape memory alloy actuators*. in *Proceedings of the 12th IASTED International Conference on Robotics and Applications*. 2006.

[33] **Sofla, A., Meguid, S., Tan, K., and Yeo, W.**, 2010. Shape morphing of aircraft wing: Status and challenges, *Materials & Design*, **31**(3), 1284-1292.

[34] **Elzey, D.M., Sofla, A.Y., and Wadley, H.N.**, 2005. A shape memory-based multifunctional structural actuator panel, *International Journal of solids and Structures*, **42**(7), 1943-1955.

[35] **Świec, P., Zubko, M., Lekston, Z., and Stróż, D.**, 2016. Structure and Properties of NiTi Shape Memory Alloy after Cold Rolling in Martensitic State, *Acta Physica Polonica A*, **130**(4), 1081-1084.

[36] **Elahinia, M.H., Hashemi, M., Tabesh, M., and Bhaduri, S.B.**, 2012. Manufacturing and processing of NiTi implants: a review, *Progress in materials science*, **57**(5), 911-946.

[37] **Otsuka, K. and Ren, X.**, 2005. Physical metallurgy of Ti–Ni-based shape memory alloys, *Progress in materials science*, **50**(5), 511-678.

[38] **Kneissl, A., Unterweger, E., Bruncko, M., Mehrabi, K., Lojen, G., and Scherngell, H.**, 2008. Microstructure and properties of NiTi and CuAlNi shape memory alloys, *Metalurgija*, **14**(2), 89-100.

[39] **Li, C.-H., Chiang, L.-J., Hsu, Y.-F., and Wang, W.-H.**, 2008. Cold Rolling-Induced Multistage Transformation in Ni-Rich NiTi Shape Memory Alloys, *Materials transactions*, **49**(9), 2136-2140.

[40] **HOLEC, D.**, 2005. On the precipitation in NiTi based shape memory alloys, Diploma thesis, Masaryk University, Brno.

[41] **Adharapurapu, R.R.**, 2007. Phase transformations in nickel-rich nickel-titanium alloys: influence of strain-rate, temperature, thermomechanical treatment and nickel composition on the shape memory and superelastic characteristics, University of California, San Diego.

[42] **Burstone, C.J. and Goldberg, A.J.**, 1980. Beta titanium: a new orthodontic alloy, *American journal of orthodontics*, **77**(2), 121-132.

[43] **Yoneyama, T. and Miyazaki, S.**, 2008. Shape memory alloys for biomedical applications, Elsevier.

[44] **Thompson, S.**, 2000. An overview of nickel–titanium alloys used in dentistry, *International endodontic journal*, **33**(4), 297-310.

[45] Lagoudas, D.C., Rediniotis, O.K., and Khan, M.M., *Applications of shape memory alloys to bioengineering and biomedical technology*, in *Scattering Theory and Biomedical Engineering Modelling and Applications*2000, World Scientific. p. 195-207.

[46] **Machado, L. and Savi, M.**, 2003. Medical applications of shape memory alloys, *Brazilian journal of medical and biological research*, **36**(6), 683-691.

[47] **Pfeifer, R., Müller, C.W., Hurschler, C., Kaierle, S., Wesling, V., and Haferkamp, H.**, 2013. Adaptable orthopedic shape memory implants, *Procedia CIRP*, **5**, 253-258.

[48] **Stoeckel, D.**, 1990. Shape memory actuators for automotive applications, *Materials & Design*, **11**(6), 302-307.

[49] **Murasawa, N., Koseki, H., Li, X.-R., Iwata, Y., and Sakamoto, T.**, 2012. Study on thermal behaviour and risk assessment of biomass fuels, *International Journal of Energy Engineering*, **2**(5), 242-252.

[50] **Cassel, B., Packer, R., and Shelton, C.**, Modulated temperature DSC and the DSC 8500: a step up in performance, *PerkinElmer, Inc. http://las. perkinelmer. com.*

[51] **Monshi, A., Foroughi, M.R., and Monshi, M.R.**, 2012. Modified Scherrer equation to estimate more accurately nano-crystallite size using XRD, *World Journal of Nano Science and Engineering*, **2**(3), 154-160.

[52] **Shiva, S., Palani, I., Mishra, S., Paul, C., and Kukreja, L.**, 2015. Investigations on the influence of composition in the development of Ni–Ti shape memory alloy using laser based additive manufacturing, *Optics & Laser Technology*, **69**, 44-51.

[53] **Davidson, M.W. and Abramowitz, M.**, 2002. Optical microscopy, *Encyclopedia of imaging science and technology*, **2**(1106-1141), 120.

[54] **Manjeri, R., Norwich, D., Sczerzenie, F., Huang, X., Long, M., and Ehrlinspiel, M.**, 2016. A study of thermo-mechanically processed high stiffness NiTiCo shape memory alloy, *Journal of Materials Engineering and Performance*, **25**(3), 894-900.

[55] **Saud, S.N., Bakar, T.A.A., Hamzah, E., Ibrahim, M.K., and Bahador, A.**, 2015. Effect of quarterly element addition of cobalt on phase transformation characteristics of Cu-Al-Ni shape memory alloys, *Metallurgical and Materials Transactions A*, **46**(8), 3528-3542.

[56] **Zu, X., You, L., Zhu, S., Wang, Z., Wu, J., and Wang, L.**, 2003. Electron-irradiation-induced Changes of martensitic transformation characteristics in TiNi shape memory alloys, *MRS Online Proceedings Library Archive*, **792**.

[57] **Kök, M. and Ateş, G.**, 2017. The effect of addition of various elements on properties of NiTi-based shape memory alloys for biomedical application, *The European Physical Journal Plus*, **132**(4), 185.

[58] **Prokoshkin, S., Korotitskiy, A., Brailovski, V., Inaekyan, K., and Dubinskiy, S.**, 2011. Crystal lattice of martensite and the reserve of recoverable strain of thermally and thermomechanically treated Ti-Ni shape-memory alloys, *The Physics of Metals and Metallography*, **112**(2), 170.

[59] **Li, W. and Zhao, C.**, 2018. Microstructure and Phase Transformation Analysis of Ni50− xTi50Lax Shape Memory Alloys, *Crystals*, **8**(9), 345.

[60] **Liang, Y., Jiang, S., Zhang, Y., and Yu, J.**, 2017. Microstructure, Mechanical Property, and Phase Transformation of Quaternary NiTiFeNb and NiTiFeTa Shape Memory Alloys, *Metals*, **7**(8), 309.

[61] Sheng, L., Yang, Y., and Xi, T. *Effect of heat treatment on morphology evolution of Ti2Ni phase in Ti-Ni-Al-Zr alloy*. in *IOP Conference Series: Materials Science and Engineering*. 2018. IOP Publishing.

[62] **Yi, H. and Moore, J.**, 1992. Combustion synthesis of TiNi intermetallic compounds, *Journal of Materials Science*, **27**(18), 5067-5072.

[63] **Yan, X., Gugel, H., Huth, S., and Theisen, W.**, 2011. Microstructures and properties of laser cladding NiTi alloy with W for biomedical applications, *Materials Letters*, **65**(19-20), 2934-2936.

[64] **Bhagyaraj, J., Ramaiah, K., Saikrishna, C., and Bhaumik, S.**, 2013. Behavior and effect of Ti2Ni phase during processing of NiTi shape memory alloy wire from cast ingot, *Journal of Alloys and Compounds*, **581**, 344-351.

[65] **Novák, P., Mejzlíková, L., Michalcová, A., Čapek, J., Beran, P., and Vojtěch, D.**, 2013. Effect of SHS conditions on microstructure of NiTi shape memory alloy, *Intermetallics*, **42**, 85-91.

[66] **Gururaja, S., Taya, M., and Kang, Y.**, 2007. Design of ferromagnetic shape memory alloy composite made of Fe and TiNi particles, *Journal of applied physics*, **102**(6), 064910.

[67] **Callister, W.D. and Rethwisch, D.G.**, 1991. Materials science and engineering: an introduction, Wiley New York.

CURRICULUM VITAE

Name: Hanaa Shahab Ahmed

Surname: Zardawi

Date of Birth: 20-Oct-1988

Place of Birth: Kifry-Iraq

Education Information: Bachelor in Physics, College of Education-Kalar, University of Sulaimani (2010-2011)

Job experience: Works in University of Garmian as lab assistant.

Publications:

International journal

1) Mediha Kök, **Hanaa Shahab Ahmed Zardawi**, Ibrahim Nazem Qader, M. Sait Kanca, The Effects of Cobalt Elements Addition on Ti2Ni Phases, Thermodynamics Paramaters, Crystal Structure and Transformation Temperature of NiTi Shape Memory Alloys **, accepted,** The European Physical Journal Plus, 2019 (SCI-Expanded)

International Congress Presentations

1) Kök, M., **Zardawi, H.S.**, Dağdelen, F., Aydoğdu, Y., NiTi Bazlı Şekil Hatırlamalı Alaşımların Fiziksel Özellikleri Üzerine Kompozisyonun Etkisi. Adım Fizik Günleri VI, (2017),-Balıkesir, Burhaniye.
2) Mediha Kök, **Hanaa Shahab Ahmead Zardawi**, Comparison of thermal, crystal and magnetic properties of NiTi and NiTi-Co shape memory alloys, CPC–XII: 12th Chemical Physics Congress 12–13 October 2018 @ Safranbolu .
3) **Hanaa Shahab Ahmead Zardawi**, Ibrahim Nazem Qader, Mediha Kök, Yıldırım Aydoğdu, The Effect of the Composition on the Transformation Temperature and Crystal Structure of NiTiCo Shape Memory Alloy, International Conference on Physical Chemistry and Functional Materials (PCFM'18)-June 19-21, 2018, Fırat University, Elazığ-Turkey.